Genotyping of Atlantic cod (*Gadus morhua*) by pantophysin I marker (Pan I)

Bachelor Thesis

October 4th, 2022

Completed at the Alfred-Wegener-Institut Bremerhaven

Author:

Caroline Withelm

Bürgermeister-Martin-Donandt Platz 22

27568 Bremerhaven

Student number: 2714070

cawithel@students.uni-mainz.de

Supervisor & first corrector: Dr. Felix Christopher Mark (AWI)

Second corrector: apl Prof. Dr. Bernhard Lieb (JGU)

Statement of Authorship

I hereby declare that I am the sole author of this bachelor thesis and that I have not used any sources other than those listed in the bibliography and identified as references.

I further declare that I have not submitted this thesis at any other institution in order to obtain a degree.

Bremerhaven, October 4th, 2022

_____

Signature

Index

Abstract

Due to climate change, the Arctic is warming twice as fast as the rest of the world. This leads to a northward expansion of species from the Atlantic to the Arctic. As a result, the species composition in the Arctic is changing. The Northeast Arctic cod (NEAC) is the most abundant cod population, with a distribution area in the Barents Sea and also in Svalbard. However, NEAC can also be found along the coast of Norway. There the NEAC spawns in the Lofoten region with the Norwegian Coastal cod (NCC), which in turn occurs along the Norwegian coast and in fjords. The offspring is drifted to Svalbard by the prevailing currents. The aim of this work was to investigate the composition of the cod population in Svalbard and whether a local coastal population has formed in Svalbard. For this purpose, the Pantophysin I locus (Pan I) was used to investigate to which ecotype of cod the caught animals from expeditions between August and October in 2018 and 2020 could be assigned. The analysis of Pan I in the caught cod shows that NCC inhabits both coastal and fjord areas in Svalbard. The discovery of NCC in Svalbard is an indication that due to climate change a coastal population may become established in Svalbard, with effects on the prevailing ecosystem in Svalbard.

Abbreviations

°C	centigrade
3'	3-prime end of DNA sequences
5'	5-prime end of DNA sequences
A	Adenin
bp	base pairs
c	concentration
C	Cytosin
$corr_f$	correction factor
DMSO	Dimethyl sulfoxide
DNA	desoxyribonucleic acid
dNTP	deoxynucleotidetriphosphate
dp	Datapoints
fwd	forward
g	force
G	Guanin
$ident_f$	identification factor
M	Molar
min	minute
NCC	Norwegian Coastal Cod
NEAC	Nordeast Arctic Cod
Pan I	pantopysin I locus
PCR	polymerase chain reaction
PCR	Polymerase Chain Reaction
rcf	relative centrifugal force
rev	reverse
rpm	rounds per minute
SciFi	scientific fishing
sec	second
T	Thymin
TL	total length
V	Volt
v	volume
YMP/SMB	Yermak Plateau/Smeerenburg

List of figures

List of tables

1 Introduction

Due to climate change, the Arctic has warmed at nearly twice the rate as the rest of the world over the last decades (NSIDC, 2020). The Svalbard archipelago, the sampling area of this thesis, is also affected by climate change and its consequences. Svalbard is influenced by cold and warm water masses of different origins. The east coast of Svalbard is influenced by cold water from the Arctic Ocean moving southwards (Spotowitz et al., 2022). The west coast of Svalbard, on the other hand, is influenced by warmer Atlantic currents. The West Spitsbergen Current (WSC), which is a branch of the gulf stream, moves northwards along the west coast (Spotowitz et al., 2022). Thus, in the region around Svalbard, Atlantic water, which is steadily warming, enters the Arctic Ocean (Onarheim et al., 2014). This increased warming will lead to changes that may affect Arctic food webs and the well-being of Arctic communities (Vincent, 2020). Due to the warming of the Arctic waters the sea ice cover is declining, opening new habitats. Since 1979, the trend in winter ice area loss is close to 10% per decade (Onarheim et al., 2014). A northward expansion of invasive species from the Atlantic, such as Atlantic cod (*Gadus morhua* (Linnaeus, 1758)), is a consequence of warming (Renaud et al., 2011; Mark et al., 2014), causing a change in species distribution and occurrence in the Arctic (Spotowitz et al., 2022).

G. morhua is a bentho-pelagic fish and distributed in the boreal regions of the North Atlantic and the Arctic (Drinkwater, F., 2005) (Figure 1).
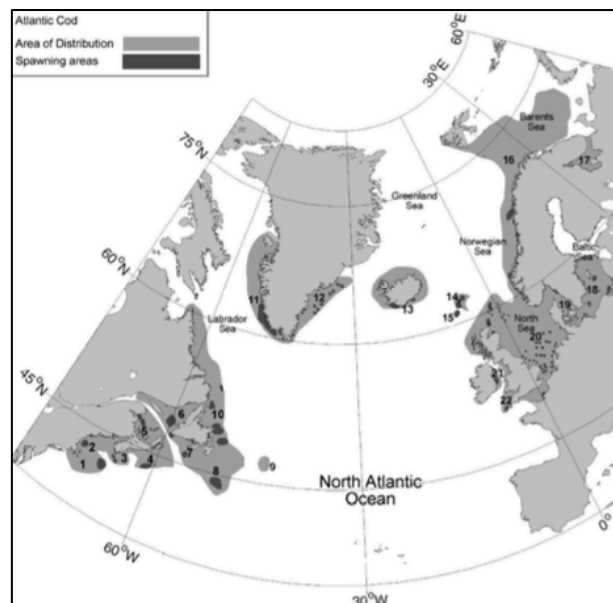
Figure 1: Distribution of Atlantic cod.
The area of distribution is shown in grey. Spawning areas are shown in dark grey. (Drinkwater, 2005).

In the North Atlantic, more precisely in the Barents Sea and in the waters along to the coast of Norway, exist two main groups of Atlantic cod. The Northeast Arctic cod (NEAC) and the Norwegian Coastal cod (NCC). Both belong to the species *Gadus morhua*. The two cod populations differ in their way of life. The NCC is more stationary along the coast of the North of Norway and is found inside fjords. The NCC spawn their eggs in different locations along the coast and inside fjords in springtime (Dahle et al., 2018; Fevolden et al., 2009). The main spawning period is from March to April (Nordeide et al., 1998). The eggs drift passively with the Norwegian Coastal Current from the spawning sites in the North of Norway to the Barents Sea until they finally are able to reach Svalbard. Now it may happen that, due to consequences of climatic changes such as the decline of sea ice, the offspring of the NCC can survive the winters in ice-free areas of fjords and, as they show less migratory behaviour (Stransky et al., 2008), they settle as a local population in the fjords and the west coast of Svalbard. Nevertheless, the NCC undertakes local coastal migrations (Berg & Albert, 2003). In contrast, the NEAC is a migratory species. They have their feeding area mainly in the Barents Sea but also along western Svalbard (Otterå et al., 2020, Andrade et al., 2020). However, its spawning area is in the North of the Norwegian coast in the region of Lofoten and Vesterålen whereto the adults of NEAC migrates between December and January (Otterå et al., 2020; Sarvas & Fevolden, 2005; Andersen et al., 2015). The offspring drift with the Norwegian Coastal Current from the coast of Norway to the northeast and mix with the Atlantic water until finally reaching the Barents Sea and Svalbard (Vikebø et al., 2005). The migratory ecotype of Atlantic cod such as the NEAC comprise the largest known cod stock compared to the NCC as a stationary population (Spotowitz et al., 2022; Markusson, H., 2020). Atlantic cod in Svalbard waters are generally assigned to the ecotype of NEAC according to the literature (Spotowitz et al., 2022). Accordingly, the spawning sites of NEAC and NCC overlap around the Lofoten during springtime (Dahle et al., 2018; Fevolden et al., 2012; Spotowitz et al., 2022; Nordeide et al., 1998). This temporary geographical overlap around the Lofoten can lead to interbreeding of the two populations and the emergence of hybrids (Stransky et al., 2008). Therefore, hybrids originate in the Lofoten region and not in Svalbard, as the NEAC has their spawning sites around the Lofoten and not in Svalbard.

As already mentioned, eggs and larvae are drifted northwards from the spawning sites in the North of Norway with the Norwegian Coastal Current finally reaching Svalbard. This also affects offspring of the NCC. There is growing evidence that a cod ecotype (NCC) that is now able to establish itself in the fjords of Svalbard due to warming will compete with native species for habitat and food, leading to a change in species composition and thus changes in the local Arctic ecosystem. Furthermore, it has already been described that cod attributed to the NCC ecotype have

also been caught in fjords on the west coast of Svalbard (Andrade et al., 2020). The interest here is whether NCC has settled permanently in Svalbard or whether this population is only temporarily resident in Svalbard (Andrade et al., 2020). Therefore, this thesis aims to investigate the population composition of Atlantic cod surveyed in Svalbard waters in 2018 as well as 2020 and whether the NCC has already established itself as a stationary coastal cod population in Svalbard due to the described consequences of climate warming. Due to the rising temperatures, there is the potential that they can survive the winter and settle in Svalbard. This could lead to perennial stocks forming and reproducing in the new habitat. The questions which emerge are: 1.) will a representative number of NCC individuals be found among the selected samples and are they already of reproductive age? It has been reported that coastal cod become mature at the age between 5 and 6 years in average (Berg & Albert, 2003). The ability of reproduce can therefore be inferred from the age. The age, in turn, can be determined by the length of the animals. Knowing that the NCC tends to be more stationary, the size of the individuals might indicate the length of stay in the respective locality. 2.) are the available data sufficient to support the statement that a costal stock of Atlantic cod (NCC) has become established at the respective locations and remains there throughout the year?

These hypotheses were tested by differentiating the selected samples, taking advantage of a specific gene locus identified in Atlantic cod in the 1990s, Pan I (Fevolden and Pogson, 1997). The gene locus (originally called GM798) codes for an integral membrane protein (Pogson, G. H., 2001), which can serve as a genetic marker for characterisation Atlantic cod ecotypes by using allele-specific PCR in combination with a subsequent fragment length analyse (Stenvik et al., 2006).

Pan I encodes part of the protein pantophysin, which is a cellular isoform of synaptophysin and occurs in neuroendocrine as well as in non-neuroendocrine tissues (Haass et al., 1996). The protein consists of four transmembrane domains, two intravesicular loops and two cytoplasmic tails (Pogson, G. H., 2001). Pan I of the Atlantic cod shows genetic differences between stationary (NCC) and migratory (NEAC) populations (Andersen et al., 2015). This allows us to determine the ecotype by genotyping the selected samples. The gene Pan I is biallelic and can be found in three different variants (Otterå et al., 2020). Figure 2 describes the three different variants in which the Pan I alleles can be present. One possible allele variant is Pan I^{AA} (blue) which shows the homozygous genotype of the Pan I^{A} allele dominating in the relatively stationary Norwegian Coastal cod (NCC). Variant 2, Pan I^{BB} (red), represents the homozygous genotype of the Pan I^{B} allele which is predominant in the migratory population of the Northeast Arctic cod (NEAC) (Felvolden & Pogson, 1997; Andersen et al., 2015). And the third variant, Pan I^{AB}, shows the heterozygous form with both alleles A and B are present, indicating the hybrid form. The different

intensities also become clear. For Pan I^{AA} and Pan I^{BB}, the intensities are clearly higher compared to the standard (orange). For Pan I^{AB}, both allele peaks have almost the same intensity.
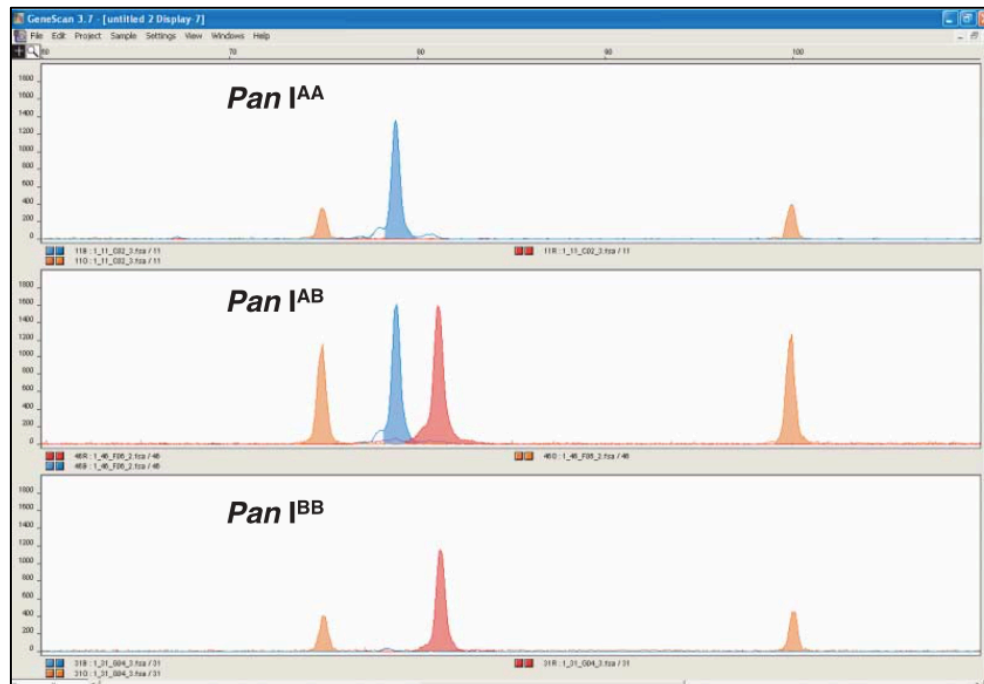
Figure 2: Pan I Genotyping.
The three different genotypes of Pan I of the Atlantic cod after fluorescent allele-specific PCR and genotyping. (Stenvik et al., 2006).

2 Material and Methods

For genotyping cod using the Pan I locus DNA is extracted, which is the DNA template for the subsequent PCR, amplifying the Pan I locus. This is done with the help of specific fluorescent-labelled reverse primers and an unmodified forward primer, flanking the region of the sequence to be amplified and serving as a starting point for the DNA polymerase. The length of these synthesised DNA fragments is then determined by fragment length analysis, which allows conclusions to be drawn about the ecotype.

2.1 Chemicals, Materials, Equipment and Media

2.1.1 Chemicals

Table 1: List of chemicals and names of their suppliers.

Name	Supplier
H_2O	AppliChem, Darmstadt, Germany
Ethanol 70%	Roth, Karlsruhe, Germany
Ethanol absolute for molecular biology	AppliChem, Darmstadt, Germany
Proteinase K	Qiagen, Venlo, Netherlands
Buffer ATL	Qiagen, Venlo, Netherlands
Buffer AL	Qiagen, Venlo, Netherlands
Buffer AW1	Qiagen, Venlo, Netherlands
Buffer AW2	Qiagen, Venlo, Netherlands
Buffer AE	Qiagen, Venlo, Netherlands
5x Phire Reaction Buffer	Thermo Scientific, Waltham, Massachusetts
Phire Hot Start II DNA Polymerase	Thermo Scientific, Waltham, Massachusetts
DMSO	Thermo Scientific, Waltham, Massachusetts
dNTPs	Roth, Karlsruhe, Germany
Primer fwd: PanI-2-PIG	Eurofins Genomics GmbH, Ebersberg, Germany
Primer rev: PanIAfam, PanIBhex	Eurofins Genomics GmbH, Ebersberg, Germany
Ultra pure Agarose	Invitrogen, Waltham, Massachusetts
Buffer TAE	AppliChem, Darmstadt, Germany
6x Orange DNA Loading Dye	Thermo Scientific, Waltham, Massachusetts
FastRuler Low Range DNA ladder	Thermo Scientific, Waltham, Massachusetts

HI-DI, Formamid	Applied biosystems, Waltham, Massachusetts
GeneScan ROX Size Standard	Applied biosystems, Waltham, Massachusetts
POP-7™ Polymer for 3730/3730xl DNA Analysers	Applied biosystems, Waltham, Massachusetts

2.1.2 Materials

Table 2: List of equipment and names of their suppliers.

Name	Supplier
2.5/10/20/100/300/1000 µl/10 ml Pipettes	Eppendorf, Hamburg, Germany
10/300 µl multichannel pipettes	Eppendorf, Hamburg, Germany
96-well reaction plate	Applied biosystems, Waltham, Massachusetts
Pipette tips, epDualfilter T.I.P.S.	Eppendorf, Hamburg, Germany
1.5/2 ml tubes	Eppendorf, Hamburg, Germany
50 ml falcon	Greiner Bio-One, Kremsmünster, Austria
tweezers	Dumont, Montignez, Switzerland
Precision wipes, Kimtech science	Kimberly-Clark, Irving, Texas

2.1.3 Equipment

Table 3: List of used equipment and names of their suppliers.

Name	Supplier
Bio Vortex V1	peQLab, Biotechnologie GmbH, Erlangen, Germany
Thermomixer comfort	Eppendorf, Hamburg, Germany
Centrifuge	Eppendorf, Hamburg, Germany
Mastercycler	Eppendorf, Hamburg, Germany
Centrifuge Galaxy Mini	VWR, Radnor, Pennsylvania
Centrifuge	SiGMA, Osterode am Harz, Germany
NanoDrop Spectrophotometer	peQLab, Biotechnologie GmbH, Erlangen, Germany
Electrophoresis, power supply	Consort, Turnhout, Belgium
Gel imager, Transilluminator	peQLab, Biotechnologie GmbH, Erlangen, Germany
Genetic Analyser 3130xl	Applied biosystems, Waltham, Massachusetts

2.1.4 Media

Table 4: List of used software and names of their suppliers.

Software and Version	Supplier
Nanodrop, ND-1000, Version 4.64.00	Thermo Scientific, Waltham, Massachusetts
VisionCapt, Version 14.2 for Windows	peQLab, Biotechnologie GmbH, Erlangen, Germany
GeneMapper, Version 4.0	Applied biosystems, Waltham, Massachusetts

2.2   Sampling area

The sampled *G. morhua* for the analysis of this thesis come from two different cruises carried out in the past years: in 2018 (cruise code: HE519) and 2020 (HE560), the cruises organized by the Alfred-Wegener-Institute (AWI) with the research vessel Heincke took place in the water around Svalbard and in its fjords. A total of 12 stations were sampled, with a total of 317 individuals surveyed (7.1.1, see appendix). The fish were partly caught by angling, but also caught with pelagic and bottom trawl. From the caught fish, among other things, muscle tissue (stored at -80°C) as well as finclips (stored in ethanol at -20°C) were taken. For this thesis, stations within fjords as well as stations from coastal and fjord areas were selected. From all stations of both cruises, a total of 7 were selected (Figure 3, Figure 4, Table 5, Table 6).

Figure 3: Selected Stations of HE519 in 2018.
Selected Stations (yellow) for this thesis of the cruise to Svalbard with Heincke (HE519) in the year 2018: S001 Bear Island, S002 Hornsund, S003 Moffen, S004/S005 Raudfjorden, S008 Kongsfjorden.

Table 5: Station details.

cruise	date	station_name	station_number	latitude	longitude
HE519	28.09.2018	Bear Island	001	74°29'36.4"N	19°30'51.6"E
HE519	29.09.2018	Hornsund	002	76°58'54.4"N	15°44'40.7"E
HE519	30.09.2018	Moffen	003	80°08'42.0"N	13°09'57.6"E
HE519	01.10.2018	Raudfjorden	004	79°47'44.8"N	12°02'58.1"E
HE519	01.20.2018	Raudfjorden	005	79°44'28.1"N	12°00'45.0"E
HE519	03.10.2018	Kongsfjorden	008	78°56'05.0"N	12°01'17.5"E
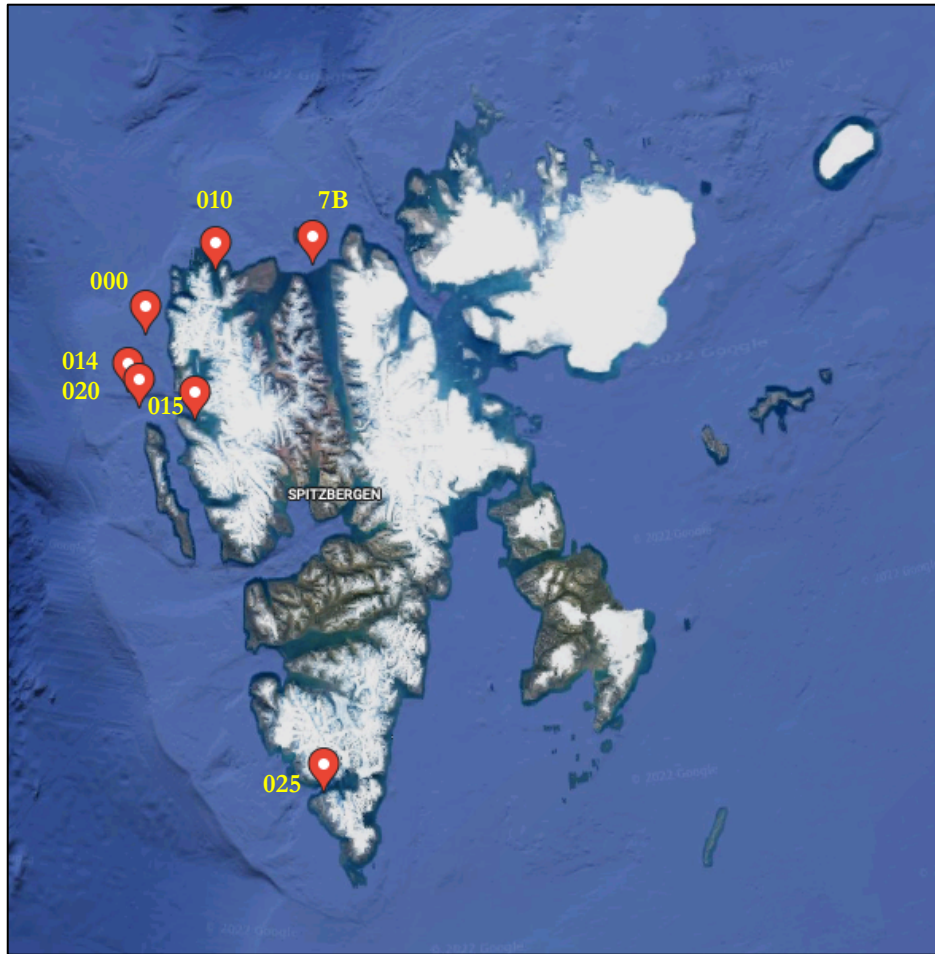
Figure 4: Selected Stations of HE560 in 2020.
Selected Stations (yellow) for this thesis of the cruise to Svalbard with Heincke (HE560) in the year 2020: S000 YMP/SMB, S010 Raudfjorden, S014 SciFi, S015/S020 Kongsfjorden, S025 Hornsund, 7B Moffen.

Table 6: Station details.

cruise	date	station name	station number	latitude	longitude
HE560	09.08.2020	YMP/SMB	000	79°24'33.8"N	10°06'09.4"E
HE560	17.08.2020	Raudfjorden	010	79°47'44.8"N	12°02'58.1"E
HE560	20.08.2020	SciFi	014	79°44'28.1"N	9°47'49.0"E
HE560	21.08.2020	Kongsfjorden	015	78°57'50.9"N	11°50'01.2"E
HE560	25.08.2020	Kongsfjorden	020	79°01'12.9"N	10°14'25.7"E
HE560	30.08.2020	Hornsund	025	76°57'02.7"N	15°48'31.8"E
HE560	14.08.2020	Moffen	7B	80°00'00.0"N	14°08'27.5"E

All individuals from these stations were sorted in ascending order of total length (TL) for each station to assign them to a size class (7.1.2, see appendix). 12 different size classes were defined. Size class *1* was assigned to individuals with total lengths between 0 and 9.9 cm, size class *2* to 10.0 to 19.9 cm etc. up to size class *12* with 110.0 to 119.9 cm total length (Figure 5). Finally, 10 individuals per station were chosen (Table A 1, see appendix). The smallest and the largest individual were selected, as well as animals in size classes in between, so that individuals of different sizes could be used for the analysis (Figure 6).

All individuals (n=38) of Bear Island assigned to size classes

All individuals (n=30) of Hornsund assigned to size classes

All individuals of Kongsfjorden assigned to size classes

All individuals (n=37) of Northwest Svalbard (region near Moffen) assigned to size classes

All individuals (n=52) of Raudfjorden assigned to size classes

All individuals (n=15) of SciFi station of the West Coast of Svalbard assigned to size classes

All individuals (n=50) of YMP/SMB assigned to size classes

Figure 5: Size classes of all Atlantic cod caught. Total of all individuals (n) of the respective selected station of both cruises assigned to their size class.

1 (0-9 cm)	**7 (60-69 cm)**
2 (10-19 cm)	**8 (70-79 cm)**
3 (20-29 cm)	**9 (80-89 cm)**
4 (30-39 cm)	**10 (90-99 cm)**
5 (40-49 cm)	**11 (100-109 cm)**
6 (50-59 cm)	**12 (110-119 cm)**

Figure 6: Size classes of Atlantic cod selected. Selected individuals (n=10) of the respective selected station of both cruises assigned to their size class.

1 (0-9 cm)	7 (60-69 cm)
2 (10-19 cm)	8 (70-79 cm)
3 (20-29 cm)	9 (80-89 cm)
4 (30-39 cm)	10 (90-99 cm)
5 (40-49 cm)	11 (100-109 cm)
6 (50-59 cm)	12 (110-119 cm)

2.3   Purification of DNA

2.3.1 DNA Extraction

DNA was extracted using a DNeasy Blood & Tissue Kit (QIAGEN). An adjusted Quick-Start protocol (April 2016) was used.
The first step of the DNA extraction was to lyse the samples with help of proteinase K.
For this step, a 1.5ml tube (Eppendorf) was prepared with 180 µl ATL buffer and 20 µl proteinase K for each sample. These were mixed by vortexing and they were then centrifuged quickly. The samples were taken under sterile conditions. For this purpose, two forceps were cleaned with 70% ethanol and then flamed with the aid of a Bunsen burner. This procedure was repeated after each sample to avoid contamination. Furthermore, a petri dish was needed for the finclips, which were also thoroughly cleaned with ethanol after each sampling.

For finclips (stored in ethanol at -20°C), attention was paid to ensure that only tissue from lower skin layers was collected to avoid possible contamination from skin surface. Therefore, the top layer of skin was lifted off and the exposed tissue was used for the extraction. Before finclip samples were transferred into the prepared lysis solution, they were carefully blotted out on a KIMTECH cloth after collection so that no ethanol remained on the tissue. Muscle samples (stored at -80°C) were transferred directly from the storage-tube into the prepared tubes with the lysis solution. The samples were then incubated at 56°C and 450 rpm overnight.

After incubation, the lysate was briefly mixed and centrifuged. In the next step, the DNA is selectively bound to the membrane of the DNeasy Mini spin column. For this, 200 µl Buffer AL was premixed with 200 µl ethanol per sample. 400 µl of the premix was added to the lysate and immediately mixed thoroughly to homogenise. The whole mixture was pipetted onto the DNeasy Mini spin column and centrifuge at 6000 x g (6.0 rcf) for 1 min. During the centrifugation, the DNA is bound to the membrane as contaminants pass through (DNeasy Blood and Tissue Handbook, QIAGEN, S.9). The flow-through and the collection tube were discarded, and the spin column was placed in a new 2 ml collection tube. In the following two wash steps, the remaining contaminations were removed. 500 µl Buffer AW1 was added onto the spin column and centrifuge at 6000 x g (6.0 rcf) for 1min. The throw-through and the collection tube were discarded. The spin column was placed in a new 2 ml collection tube. 500 µl Buffer AW2 was added onto the spin column and centrifuge at 16.100 x g (16.1 rcf) for 3 min. The collection tube was emptied and blotted, then the spin column was placed back onto the collection tube and centrifuge again at 16.100 x g (16.1 rcf) for 1 min. The collection tube including flow-through was discarded and the spin column was transferred to a new 1.5 ml microcentrifuge tube. To elute the DNA from the membrane of the DNeasy Mini spin column, 150 µl Buffer AE was pipetted to the center of the

spin column membrane and incubate at room temperature for 1 min. After incubation, centrifuged at 6000 x g (6.0 rcf) for 1 min. The spin column was discarded. The DNA is eluted in the buffer.

2.3.2 Quantification of the purified DNA

To determine the yield of the extracted DNA the concentration was measured a Nanodrop Spectrophotometer. The absorbance peak of DNA is at 260nm, that of proteins at 280nm. The ratio of absorbance at 260 and 280 nm provides information about the purity of the measured DNA. DNA is considered pure when the ratio is ~1,8. If the ratio is clearly below 1,8, this may indicate contamination, for example by protein.

So that the measurement of the DNA concentration is not falsified by the absorbance values of the buffer, a previous reference measure is necessary, which is carried out with buffer AE in which the DNA is eluted. After blanking, the DNA concentration (ng/µl) of all samples was quantified (Table A 2, see appendix). The purified DNA samples were then diluted in distilled water to an end concentration of 10 ng/µl with a final volume of 50 µl. For this purpose, the following formulas were used:

To determine the needed volume of the eluted DNA:

$$v_1 = \frac{c_2 (end\ concentration) * v_2 (endvolume)}{c_1 (concentration\ of\ the\ purified\ DNA)}$$

To determine the needed volume of H_2O:

$$v_{H2O} = v_2 - v_1$$

The pure DNA as well as the diluted DNA were immediately stored at -20°C.

2.4   Allele-specific Polymerase Chain Reaction

By using PCR, specific DNA sequences can be amplified *in vitro* (Sadava et al., 2006). PCR was performed to amplify the Pan I locus and to identify in a subsequent fragment analysis, if one or both alleles of the locus are present. For this purpose, two different fluorescent-labelled reverse primers, specific for Pan I^{A} (PanIAfam-R) or Pan I^{B}(PanIBhex-R), and one unlabelled forward primer (PanI-2-PIG), flanking the searched locus and serving as a starting point for the polymerase, were used (Table 7). The fluorescent primers allow a specific amplification of the Pan I locus in PCR (Stenvik et al., 2006). The forward primer was modified by a PIG-tail. This means that a sequence is added to the 5'end, in our case the sequence GTTTCTT (Table 7). The PIG-tailing modification is intended to improve the genotyping (Brownstein et al., 1996).

Table 7: PCR primer list.
Primers with their respective sequences and band sizes. PIG-tail sequence underlined.

Primer name	Sequence (5'-> 3')	Band size in Bp
PanI-2-PIG	<u>GTTTCTT</u>TGACAGCGCTTGGCAAATGAA	28
PanIAfam-R	GCTTAAGCAGATATCGCAGTAGTTTC	26
PanIBhex-R	TTAAGCAGATCTCCGCAGTAGTTTT	24

The final volume of the PCR mix was 20 µl per sample consisting of 18,5 µl PCR reaction mix and 1,5 µl template DNA. The total volume was determined according to the number of samples. All volumes of the required components were determined according to the supplier's information (Table 8) in relation to the calculated total volume for the reaction mix. The amount of water was determined proportionally from the sum of these. Two PCR reaction mixtures were prepared, each with one of the two primers since it was decided against a multiplex PCR during the pretests.
Starting with water, all components were pipetted in order 1-6 (Table 8) into a reaction tube and mixed by vortexing. Finally, PCR reaction tubes were prepared with 18,5 µl of the reaction mix and 1,5 µl of the template DNA.

Table 8: Pipetting instructions.

Order	Component	Stock concentration	Final concentration
1	Phire Reaction Buffer	5X	1X
2	dNTPs	2 mM	0,2 mM
3	Primer fwd	100 μM	0,5 μM
4	Primer rev	100 μM	0,5 μM
5	DMSO	-	0,6 μl/reaction
6	Phire Hot Start II DNA Polymerase	-	0,4 μl/reaction

A Mastercycler was used for the Polymerase Chain Reaction. After an initial denaturation step for 30 sec at 98°C, 30 cycles of DNA amplification followed. The DNA is heated to 98°C for 5 sec, whereby the single strands separate. The denaturation is followed by primer annealing at 64°C for 5 sec. In this step, the primers bind to their target sequence (Sadava et al., 2006). In the following extension step with a temperature of 72°C for 10 sec the DNA polymerase synthesizes the new complementary strands, using the dNTPs as building blocks (Sadava et al., 2006). Once the 30 cycles are completed, the process ends with the final extension at 72°C for 1 min and the subsequent final hold at 4°C. During the reaction, the buffer regulates the pH value (Sadava et al., 2006) to guarantee optimal conditions for the activity and stability of the DNA-polymerase (Gelfand, 1989).

2.5   Gel electrophoresis

To verify whether the PCR worked, which means the primer successfully bind to their target region, a gel electrophoresis was run. According to the literature, the size of the products determined by fragment analysis is 79 bp for Pan I^A und 77 bp for Pan I^B, so a band just above the 50 bp band of the DNA ladder should be visible in our gel.

A 3% (weight/volume) Agarose gel was produced by dissolving 3 g Agarose in 100 ml TAE (Tris-acetate-EDTA) buffer. The mixture was heated up until a homogeneous solution was obtained. When the solution was cooled down, it was poured to a gel tray equipped with gel combs. After polymerisation of the solution, the gel tray was transferred into the electrophoresis chamber filled with TAE-buffer. Afterwards the gel combs were removed so that the gel was ready for sample application. To prepare the PCR products for the gel electrophoresis, 1 µl DNA Loading Dye was placed into a reaction plate and 4 µl PCR product was added.

All samples were pipetted into the lanes and finally 3 µl of the DNA ladder was applied. The electrophoresis chamber was connected to a power supply and the gel run for 35 min at 100 V.

For visualisation of the gel a transilluminator was used. The gel was placed into a staining solution to make the DNA fragments visible in form of bands by UV light.

2.6   DNA Fragment length analysis

2.6.1   Capillary electrophoresis using Genetic Analyser 3130xl (Applied biosystems)

By using fragment analysis, the size of fluorescent-labelled DNA fragments can be determined. The fragments are separated by capillary electrophoresis, whose capillaries are filled with polymer, and detected by laser, whereby the exact size in bp is determined by comparison with a size standard. This genetic analysis method was used to find out in the subsequent evaluation whether the allele exists homozygous or heterozygous, which then allowed us to determine the ecotype.

To prepare the PCR products for the fragment length analysis, they were first diluted 1:20 in distilled water. Then a mixture of 15 µl per sample of HiDi and 0,3 µl per sample of ROX size standard was prepared. Afterwards, 15 µl of the HiDi-ROX-mix and 1 µl of the diluted PCR product were pipetted into a 96-well plate and directly denatured at 95°C for 5 min. Before the plate was placed into the Genetic Analyser, it was cooled in a cooling rack. One run for 16 samples took 90 min.

2.6.2 GeneMapper Software

If the labeled primer has bound to the target region of the DNA during PCR and the respective products synthesized, the labelled products could then be detected by the laser of the Genetic Analyser. The GeneMapper Software was then used to illustrate and analyse the results. To be able to analyse the products, a new analysis method was created as described in the manual of the GeneMapper Software (Thermo Fisher Scientific, 2009). The allele and marker definitions including the fragment size (bp) and the dye colour for both were defined and adjusted.

The size standard ROX75 indicates a peak at a length of 75 bp. It represents a reference point to which the peaks of the labelled Pan I allele sequences are related. On the one hand, this allows the length (bp) of the products to be inferred. On the other hand, the relation between the intensity or height of the standard peak and that of the products can be used to determine whether the allele is homozygous or heterozygous, as described above.

Accordingly, the important information was the intensity of the Peak (height in datapoints) and the length of the fragment (bp). Based on these data, conclusions could be drawn in which variants the alleles were present. Therefore, a sizing table was created, which displays a row of sizing information for each detected peak (Applied Biosystems, 2009). The data of the height of the peak and the base pair length of the labelled products were taken from the sizing table of the Gene Mapper Software. An Excel table was created based on this sizing table (7.1.3, see appendix).

2.7   Correction of the raw data

As already described, the value of ROX75 intensity is the reference point to which the intensities of the allele peaks are referred. This means that the intensities of the allele peaks are considered in relation to the intensity of ROX75. It is therefore important that ROX75 has the same value in all samples so that the allele intensities linked to the standard by the ratio can be compared with each other. Since the two primers for the Pan I alleles were used separately in the PCR, two fragment analysis results were available for each sample in which ROX75 did not always have the same intensity value. This also occurred when the results of the intensities of the different samples were compared with each other. Therefore, it was necessary to adjust the data using correction factors for comparability.

2.7.1   Correction of the intensity values

In order to firstly compare the data for each sample of the identical DNA and secondly that all samples can be compared with each other, the intensity value of ROX75 was set to the value 500 for all samples. Thus, the measured intensity values of the alleles also had to be adjusted to the newly determined ROX75 value (ROX75$_{corr}$) so that the ratio of intensity between ROX75 and the alleles is maintained. In the following, this new value of the ratio is called 'correction factor' (corr$_f$).

The fragment analysis results of sample GmoH025 were used for the following calculation example:

Results of GmoH025 for Pan I^A:

Table 9: Results of the fragment length analysis for GmoH025 for allele Pan I^A.

Intensity of the ROX75 (in dp)	Intensity of the Pan I^A (in dp)
844	642

First, the ratio of the ROX$_{corr}$ value of 500 dp to the measured value of Pan I^A was calculated:

Definition of corr$_f$ for Pan I^A:

$$corr_f(Pan\ I^A) = \frac{ROX75_{corr}}{Pan\ I^A\ intensity}$$

Calculation of corr$_f$(Pan I^A):

$$corr_f(Pan\ I^A) = \frac{500}{844} = 0{,}59241706$$

Next, the corr$_f$(Pan I^A) was applied to the measured value of Pan I^A allele intensity to determine the new intensity (Pan I^{A}corr) relative to the ROX75$_{corr}$ intensity value of 500 dp, so that the ratio of the two values remains the same even though the ROX75 value is new.

For this purpose, the following calculation was used:

Definition of Pan I^{A}corr:

$$Pan\ I^A corr = corr_f(Pan\ I^A) \times Pan\ I^A\ intensity$$

Calculation of Pan I^{A}corr:

$$Pan\ I^A corr = 0{,}59241706 \times 642 = 380{,}331754$$

Results of GmoH025 for Pan I^B:

Table 10: Results of the fragment length analysis for GmoH025 for allele Pan I^B.

Intensity of the ROX75 (in dp)	Intensity of the Pan I^B (in dp)
675	1139

Definition of corr$_f$ for Pan I^B:

$$corr_f(Pan\ I^B) = \frac{ROX75_{corr}}{Pan\ I^B\ intensity}$$

Calculation of corr$_f$(Pan I^B):

$$corr_f(Pan\ I^B) = \frac{500}{675} = 0{,}74074074$$

Definition of Pan I^{B}corr:

$$Pan\ I^B corr = corr_f(Pan\ I^B) \times Pan\ I^B\ intensity$$

Calculation of Pan I^{B}corr:

$$Pan\ I^B corr = 0{,}74074074 \times 1139 = 843{,}703704$$

The data of Pan I^Acorr and Pan I^Bcorr obtained in this way were rounded to the nearest integer:

Table 11: New values of ROX75, Pan I^A and I^B of GmoH025.

Intensity of the ROX75$_{corr}$ (in dp)	Intensity of the Pan I^Acorr (in dp)	Intensity of the Pan I^Bcorr (in dp)
500	380	844

In this way, the intensity values of all samples were corrected (Table A 3, Table A 4, see appendix).

2.7.2 Determination of an identification factor

Since, as already mentioned, heterozygosity or homozygosity is determined, among other things, by comparing the height of the peak (intensity) of the alleles with the standard and the values of the intensities of the two Pan I alleles are already related to the standard as a reference point. The evaluation could be carried out by looking at the ratios of the intensities.

The results of the fragment length analysis of this project, differed from those described in the literature as follows. There were results (n=30) that showed a single peak and thus allowed a clear ecotype assignment. However, the remaining results (n=40) deviated from the results in the literature to the effect that even though these samples showed a peak at the location of allele A and a peak at the location of allele B, but the ratios of the two peaks did not clearly point to the third allele variant (heterozygosity). Therefore, an additional calculated factor had to be introduced, which nevertheless allows the deviating results to be interpreted. This is referred to as the "identification factor" (ident$_f$) in the following. Ident$_f$ indicates how much higher or lower the intensity of the Pan I^Acorr allele is compared to the Pan I^Bcorr allele, i.e., the intensity ratio of Pan I^Acorr : Pan I^Bcorr is.

The following example calculation is intended to illustrate the $ident_f$ explained in the previous section. The corrected values of sample GmoH025 are used for the calculation (see above).

Definition of $ident_f$:

$$ident_f = \frac{Pan\ I^A corr}{Pan\ I^B corr}$$

Calculation of $ident_f$:

$$ident_f = \frac{380}{844} = 0,45$$

In this way, $ident_f$ of all samples were calculated (Table A 5, see appendix).

The $ident_f$ could then be used to decide which of the three possibilities of the Pan I genotype was applicable. Ranges were defined for this purpose.

Homozygosity:

Variant 1 Pan I^{AA}: From an $ident_f$ of 2.0, the individuals are assigned to the NCC ecotype. This means that from a ratio of the intensity of the Pan I^A allele to that of the Pan I^B allele of 2:1, homozygosity for Pan IA is determined.

Variant 2 Pan I^{BB}: An $ident_f$ of 0.5 or smaller, in other words, if the ratio between the intensity of the Pan I^A allele and that of the Pan I^B allele is at maximum 1:2, homozygosity for Pan I^B is defined thus the individual belongs to the ecotype of the NEAC.

Heterozygosity:

Variant 3 Pan I^{AB}: If the calculated $ident_f$ is between 0.51 and 1.99, the individual is assumed to have a heterozygous genotype and is thus assigned to the group of hybrids.

3 Results

3.1 Genotype plots

In this project, the genotyping was performed in order to determine the ecotype of the collected samples. The two different fluorescent primers specific for Pan I were detected by the laser of the Genetic Analyser 3130xl. If the allele was present, this was displayed in form of a peak in position of the respective base pair length with 77 bp for Pan I^B and 79 bp for Pan I^A. Fragments from three individuals (GmoH56, GmoH057 and GmoH049) are shown below (Figure 7-9).
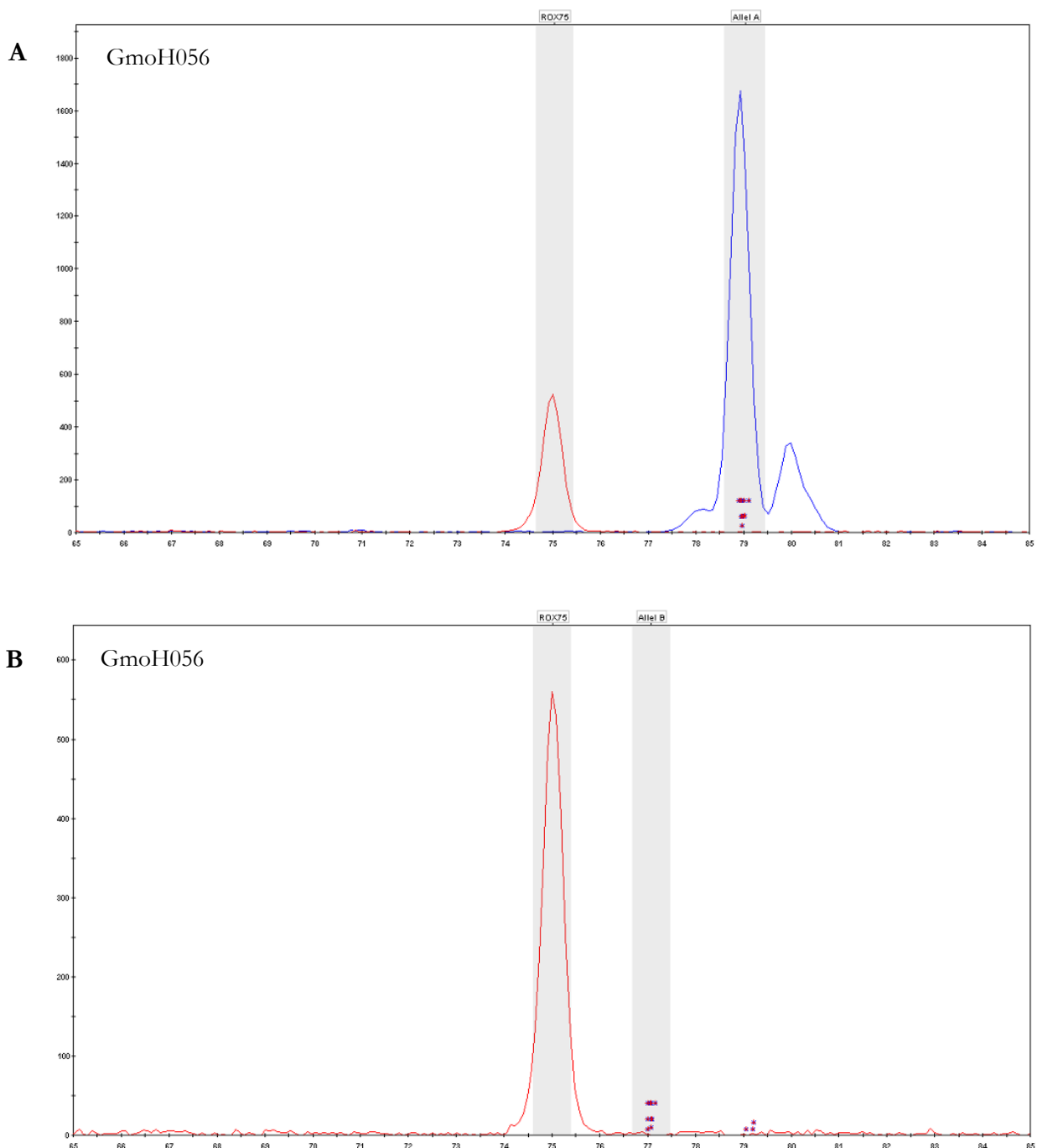
Figure 7: Genotype plots of the homozygous genotype PanI^{AA}.
A: Genotyping results of PCR product using primer for Pan I^A. B: Genotyping results of PCR product using primer for Pan I^B. Y-axis: intensity (in dp). X-axis: fragment length (in bp).
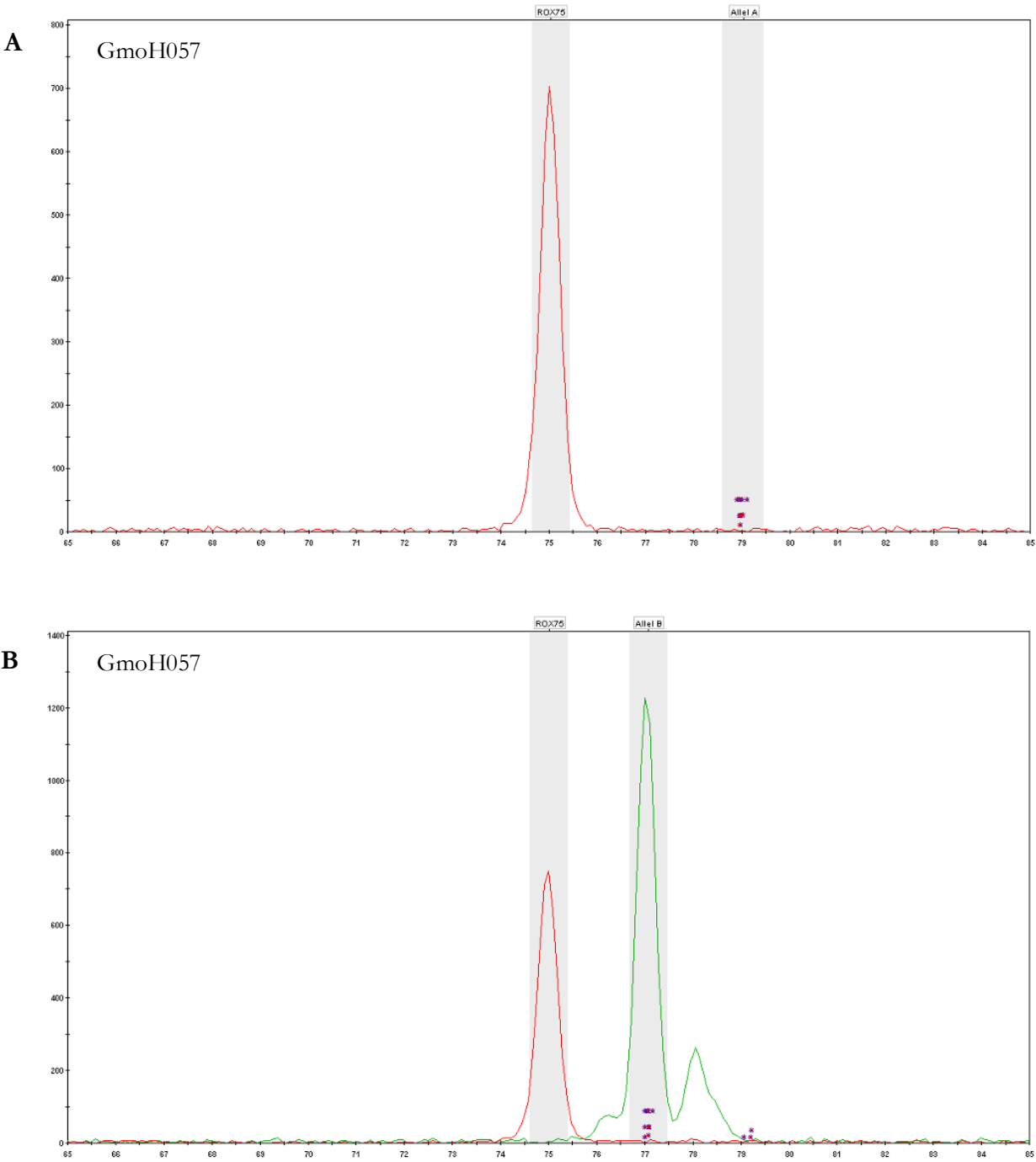
Figure 8: Genotype plots of the homozygous genotype PanI^{BB}.
A: Genotyping results of PCR product using primer for Pan I^A. B: Genotyping results of PCR product using primer for Pan I^B. Y-axis: intensity (in dp). X-axis: fragment length (in bp).
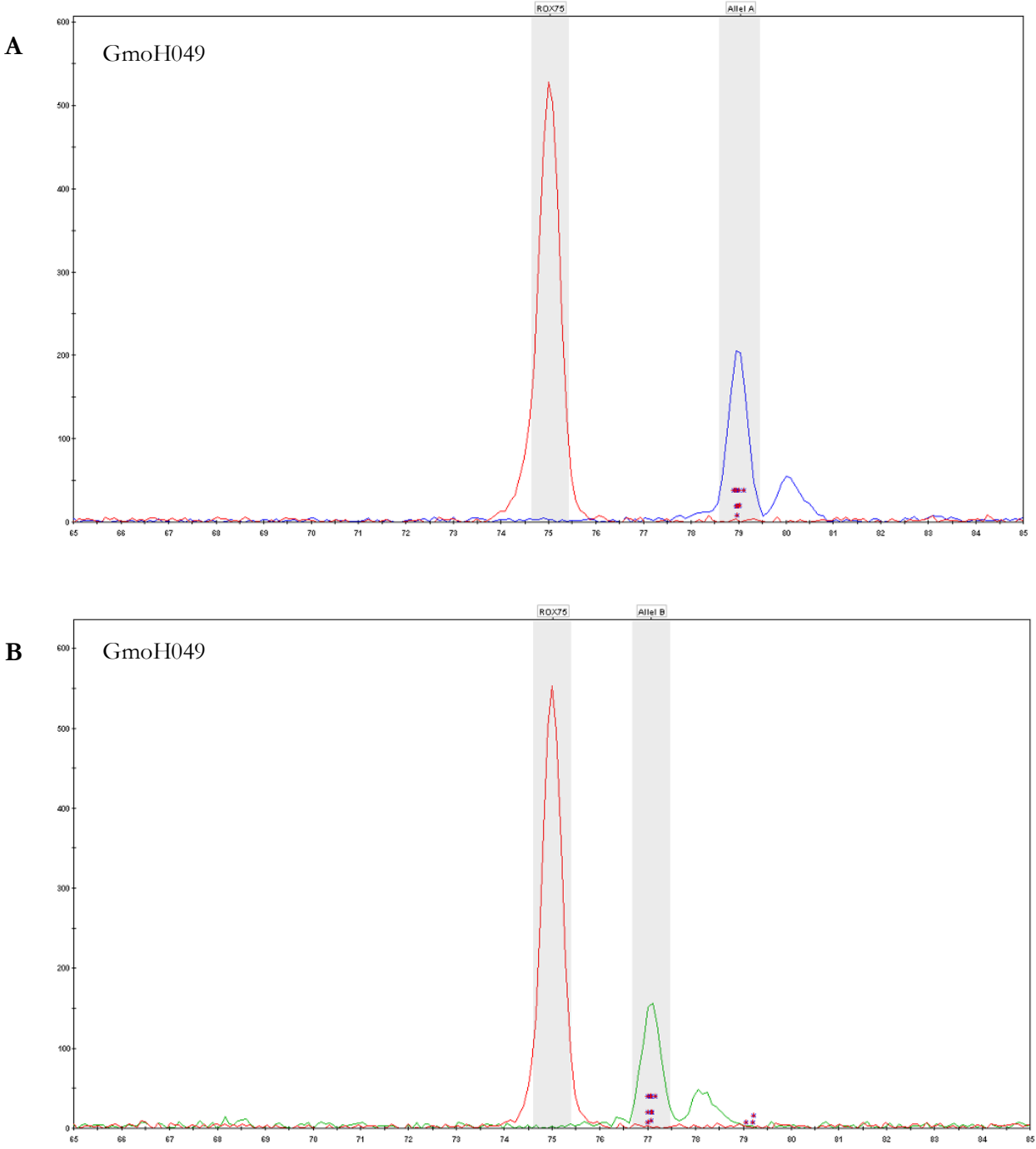
Figure 9: Genotype plots of the heterozygous genotype PanI^{AB}.
A: Genotyping results of PCR product using primer for Pan I^{A} locus. B: Genotyping results of PCR product using primer for Pan I^{B} locus. Y-axis: intensity (in dp). X-axis: fragment length (in bp).

3.2 Ecotype determination

As already described, the ecotype determination was carried out with the help of the calculated identification factor (ident$_f$). Ident$_f$ indicates the ratio of the intensity of the Pan I^A allele to that of the Pan I^B allele, both are related to the ROX75$_{corr}$ Standard. Ranges were determined for the three possible variants of how the alleles can be present. Using this information, it was discovered that of the 70 samples, 24 can be attributed to the ecotype of the NCC (Figure 10, Table 12). 37 individuals belong to the ecotype of the NEAC (Figure 10 ,Table 13) and 9 have both Pan I alleles and are thus hybrids (Figure 10, Table 14).
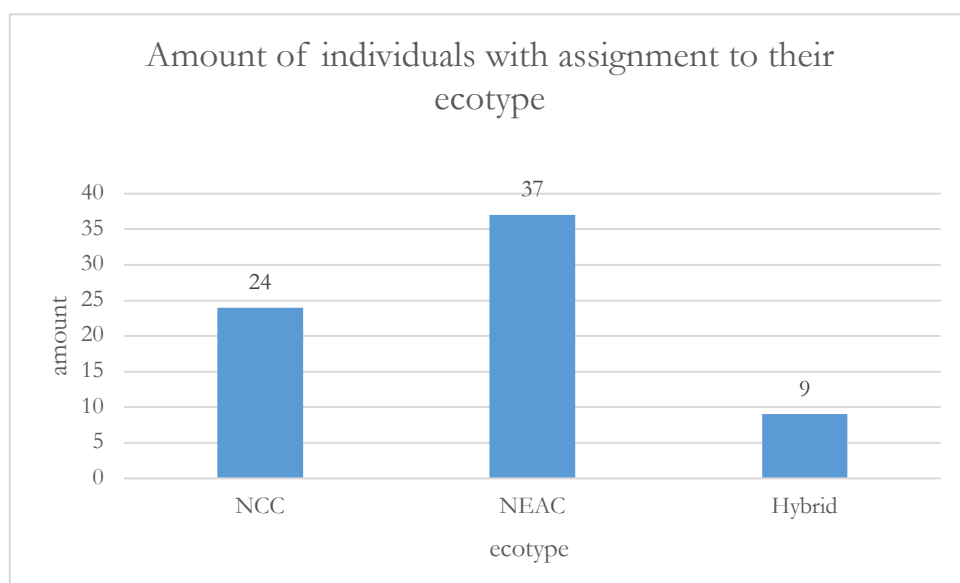
Figure 10: All tested samples assigned to their ecotype.

Table 12: Samples with the genotype Pan I^{AA} belonging to the ecotype of NCC.
Identified by evaluating a calculated relation factor (ident$_f$). Sorted by ident$_f$ (ascending).

Id	Cruise	Station N°	Pan I^{A}corr	Pan I^{B}corr	ident$_f$	Allel	Ecotype
			(intensity)	*(intensity)*	*(Pan I^A corr/Pan I^B corr)*		
GmoH070	HE519	002	183	83	2,21	Pan I^{AA}	NCC
GmoH083	HE560	7B	439	193	2,28	Pan I^{AA}	NCC
GmoH062	HE519	001	296	107	2,75	Pan I^{AA}	NCC
GmoH044	HE519	008	1464	533	2,75	Pan I^{AA}	NCC
GmoH046	HE519	003	347	125	2,78	Pan I^{AA}	NCC
GmoH063	HE519	001	298	91	3,27	Pan I^{AA}	NCC
GmoH055	HE560	000	1349	403	3,34	Pan I^{AA}	NCC
GmoH079	HE519	005	553	157	3,53	Pan I^{AA}	NCC
GmoH053	HE560	000	1037	261	3,98	Pan I^{AA}	NCC
GmoH041	HE560	000	887	220	4,04	Pan I^{AA}	NCC
GmoH051	HE519	004	456	86	5,31	Pan I^{AA}	NCC
GmoH077	HE519	008	8552	144	5,91	Pan I^{AA}	NCC
GmoH028	HE560	014	2078	338	6,15	Pan I^{AA}	NCC
GmoH099	HE560	014	2617	346	7,55	Pan I^{AA}	NCC
GmoH095	HE560	014	2482	325	7,63	Pan I^{AA}	NCC
GmoH056	HE560	000	1592	0	-	Pan I^{AA}	NCC
GmoH061	HE560	000	1976	0	-	Pan I^{AA}	NCC
GmoH065	HE519	001	291	0	-	Pan I^{AA}	NCC
GmoH048	HE519	003	117	0	-	Pan I^{AA}	NCC
GmoH092	HE560	014	1146	0	-	Pan I^{AA}	NCC
GmoH093	HE560	014	1610	0	-	Pan I^{AA}	NCC
GmoH094	HE560	014	1484	0	-	Pan I^{AA}	NCC
GmoH096	HE560	014	2981	0	-	Pan I^{AA}	NCC
GmoH098	HE560	014	4696	0	-	Pan I^{AA}	NCC
							Σ=24

Table 13:Samples with the genotype Pan I^{BB} belonging to the ecotype of NEAC.
Identified by evaluating a calculated relation factor (ident$_f$). Sorted by ident$_f$ (ascending).

Id	Cruise	Station N°	Pan I^{A}corr (intensity in Dp))	Pan I^{B}corr (intensity in Dp)	ident$_f$ (Pan I^A corr/Pan I^B corr)	Allel	Ecotype
GmoH025	HE519	001	380	844	0,45	Pan I^{BB}	NEAC
GmoH068	HE519	001	1018	3554	0,28	Pan I^{BB}	NEAC
GmoH037	HE519	008	50	179	0,28	Pan I^{BB}	NEAC
GmoH080	HE519	005	160	680	0,23	Pan I^{BB}	NEAC
GmoH031	HE519	001	53	887	0,06	Pan I^{BB}	NEAC
GmoH027	HE519	008	30	664	0,05	Pan I^{BB}	NEAC
GmoH084	HE560	7B	0	786	0	Pan I^{BB}	NEAC
GmoH085	HE560	7B	0	605	0	Pan I^{BB}	NEAC
GmoH086	HE560	7B	0	440	0	Pan I^{BB}	NEAC
GmoH087	HE560	7B	0	450	0	Pan I^{BB}	NEAC
GmoH054	HE560	000	0	453	0	Pan I^{BB}	NEAC
GmoH057	HE560	000	0	818	0	Pan I^{BB}	NEAC
GmoH059	HE560	000	0	5540	0	Pan I^{BB}	NEAC
GmoH060	HE560	000	0	718	0	Pan I^{BB}	NEAC
GmoH066	HE519	001	0	851	0	Pan I^{BB}	NEAC
GmoH033	HE519	002	0	205	0	Pan I^{BB}	NEAC
GmoH052	HE519	002	0	52	0	Pan I^{BB}	NEAC
GmoH069	HE519	002	0	120	0	Pan I^{BB}	NEAC
GmoH071	HE519	002	0	53	0	Pan I^{BB}	NEAC
GmoH072	HE519	002	0	59	0	Pan I^{BB}	NEAC
GmoH073	HE519	002	0	50	0	Pan I^{BB}	NEAC
GmoH074	HE519	002	0	316	0	Pan I^{BB}	NEAC
GmoH047	HE519	003	0	115	0	Pan I^{BB}	NEAC
GmoH082	HE519	003	0	896	0	Pan I^{BB}	NEAC
GmoH035	HE519	004	0	122	0	Pan I^{BB}	NEAC
GmoH050	HE519	004	0	510	0	Pan I^{BB}	NEAC
GmoH078	HE519	005	0	738	0	Pan I^{BB}	NEAC
GmoH045	HE519	008	0	737	0	Pan I^{BB}	NEAC
GmoH075	HE519	008	0	223	0	Pan I^{BB}	NEAC
GmoH076	HE519	008	0	548	0	Pan I^{BB}	NEAC
GmoH088	HE560	010	0	444	0	Pan I^{BB}	NEAC
GmoH089	HE560	010	0	580	0	Pan I^{BB}	NEAC
GmoH090	HE560	010	0	764	0	Pan I^{BB}	NEAC
GmoH081	HE560	015	0	665	0	Pan I^{BB}	NEAC
GmoH029	HE560	020	0	19391	0	Pan I^{BB}	NEAC
GmoH030	HE560	025	0	1111	0	Pan I^{BB}	NEAC
GmoH040	HE560	025	0	521	0	Pan I^{BB}	NEAC
							Σ=37

Table 14: Samples with the genotype Pan I^{AB} which represents the hybrid form.
Identified by evaluating a calculated relation factor (ident$_f$). Sorted by ident$_f$ (ascending).

Id	Cruise	Station N°	Pan I^{A}corr	Pan I^{B}corr	ident$_f$	Allel	Ecotype
			(intensity)	*(intensity)*	*(Pan I^A corr/Pan I^B corr)*		
GmoH064	HE519	001	477	937	0,51	Pan I^{AB}	Hybrid
GmoH026	HE519	004	240	289	0,83	PanI^{AB}	Hybrid
GmoH067	HE519	001	277	215	1,29	PanI^{AB}	Hybrid
GmoH049	HE519	003	194	141	1,38	PanI^{AB}	Hybrid
GmoH058	HE560	000	583	417	1,4	PanI^{AB}	Hybrid
GmoH043	HE519	008	502	298	1,69	PanI^{AB}	Hybrid
GmoH097	HE560	014	1555	876	1,78	Pan I^{AB}	Hybrid
GmoH091	HE560	014	798	447	1,79	Pan I^{AB}	Hybrid
GmoH042	HE519	001	265	139	1,91	Pan I^{AA}	NCC
							Σ=9

3.3   Size and age classes of the individuals belonging to Norwegian Coastal cod

As already described, it is assumed that NCC are rather loyal to their location and do not migrate over long distances. In the following, the size classes of the individuals assigned to the ecotype of NCC are presented below. The size will be used to classify the age of the individuals (reference values see Figure 11). This data can be used to make an assumption about how long the animals have already been at the sites and whether a statement can be made about the possibility of the NCCs found being an established local cod population in Svalbard.
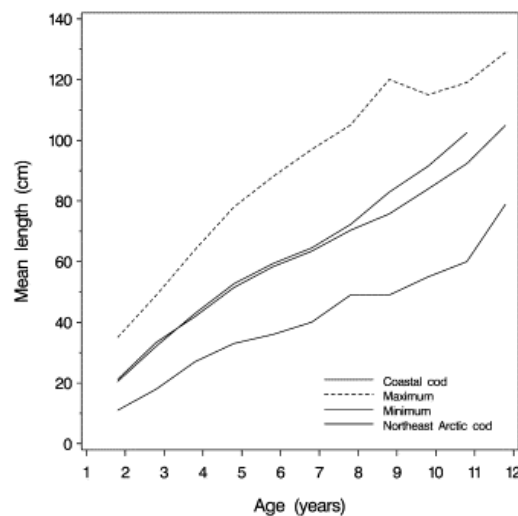
Figure 11: Length at age.
"Mean, minimum, and maximum length at age for coastal cod and Nordeast Arctic cod, 1995-2001 combined. […]" (Berg & Albert, 2003).

3.3.1 Size classes

In this section, the size classes of the three different ecotypes identified are presented for the purpose of completeness. For the discussion of the possible population relocation of the NCC that follows, however, only the presented information on size classes of the NCC (Figure 12A) is used. The length of the smallest individual of NCC is 19 cm, that of the largest 101 cm, on average the length is 71,96 cm. For NEAC the average length is 50,59 cm, the smallest in size class 2 is 13 cm and the length of the largest individual is 110 cm assigned to size class 11 (Figure 12B). Length of the smallest in size class 6 of the hybrid group is 53 cm, the largest is 89 cm. Mean length is 70,22 cm (Figure 12C).

A Size classes of individuals assigned to NCC (=24)

B Size classes of individuals assigned to NEAC (n=37)

C Size classes of individuals assigned to the group of hybrids (n=8)

Figure 12: Size classes of NCC (A), NEAC (B) and Hybrids (C).

1 (0-9 cm)	7 (60-69 cm)
2 (10-19 cm)	8 (70-79 cm)
3 (20-29 cm)	9 (80-89 cm)
4 (30-39 cm)	10 (90-99 cm)
5 (40-49 cm)	11 (100-109 cm)
6 (50-59 cm)	12 (110-119 cm)
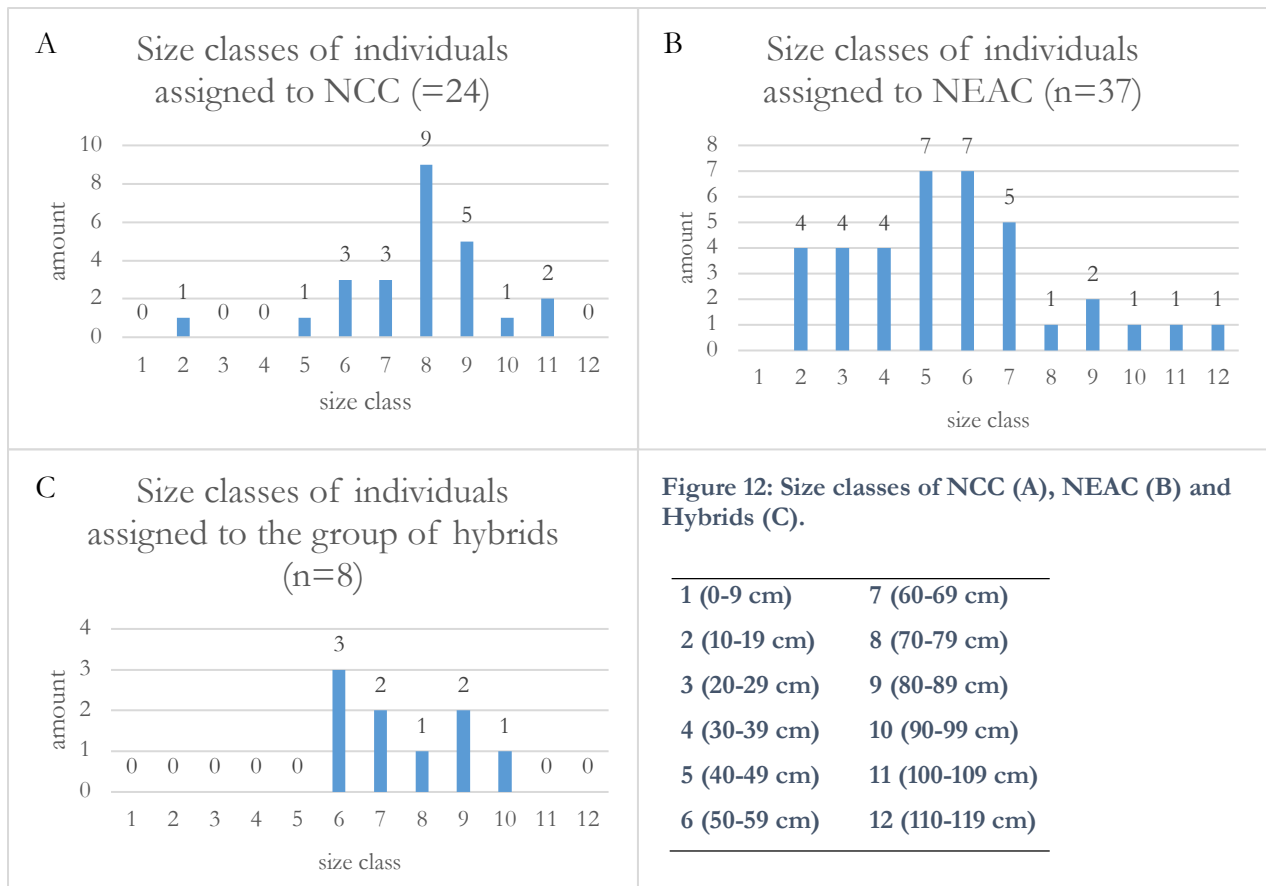
3.3.2 Age classes

In this section, the age classes of the three different ecotypes identified are presented for the purpose of completeness. For the interpretation that follows, however, only the presented information on age classes of the NCC is used. The youngest individual of NCC in age class 1 is in the 0-year group, the oldest 10-11 years old in age class 10 (Figure 13A). Mean age of NCC is 7 years. The average age of NEAC is between 4 and 5 years. The youngest individuals are in age class 1. The oldest is in age class 11, therefore over 11 years old (Figure 13B). Mean age of the hybrid group is 7 years. Youngest individuals are in age class 5, the oldest in age class 9 (Figure 13C).

Figure 13: Age classes of NCC (A), NEAC (B) and Hybrids (C).
(x-axis: the associated size classes in brackets)

1 (0-group)	7 (7-8 years)
2 (2-3 years)	8 (8-9 years)
3 (3-4 years)	9 (9-10 years)
4 (4-5 years)	10 (10-11 years)
5 (5-6 years)	11 (>11 years)
6 (6-7 years)	
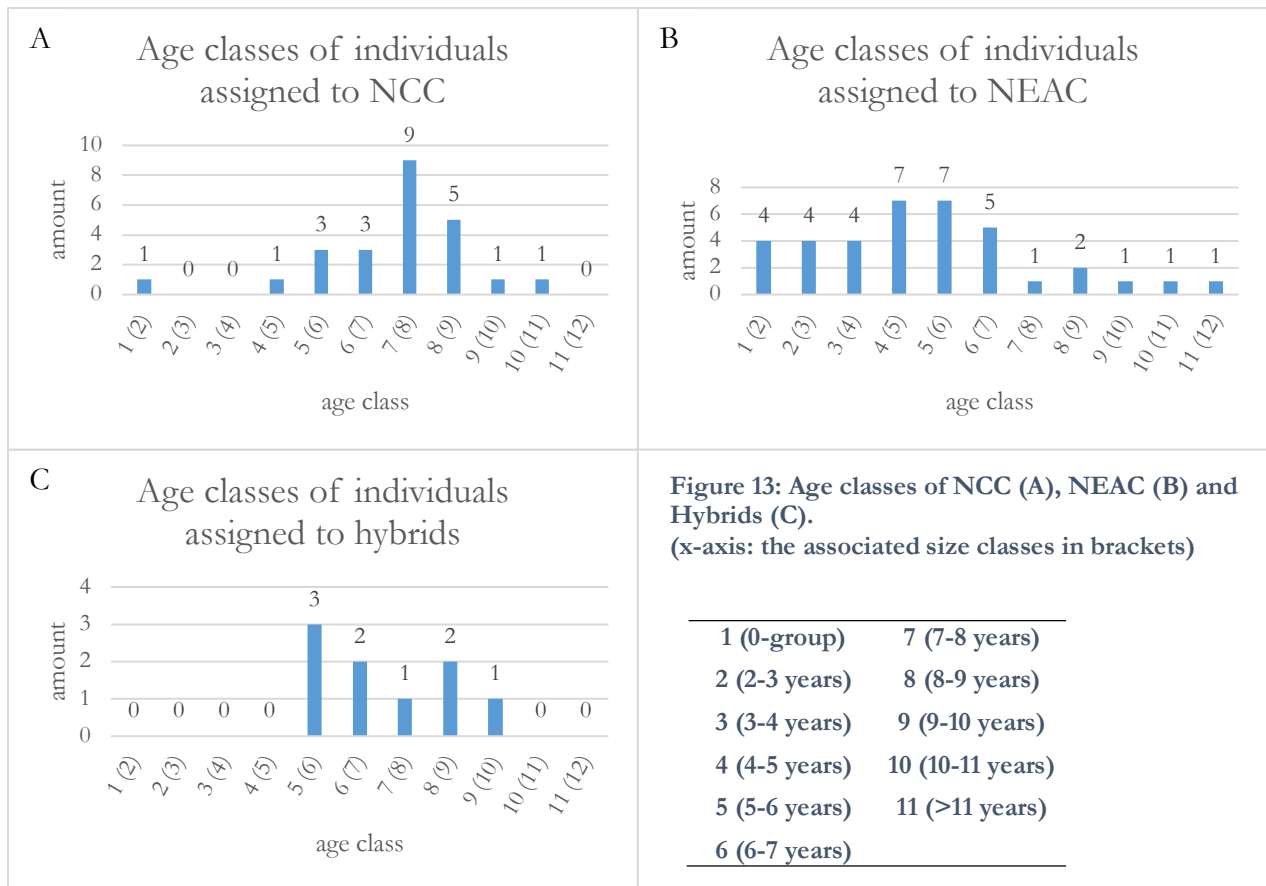
3.4 Ecotype distribution in relation to locality

In order to make a statement about the locality of the different ecotypes, the results of the determination were assigned to the locations. A differentiation was made between coastal areas and areas within fjords. The differentiation according to the stations selected for this work follows. On this basis of these results concerning the whereabouts, it can be checked with help of ice maps whether the animals found, assigned to ecotype NCC, could have spent the winter at the respective station (Figure A 1-10, see appendix). Based on this, a possible migration behaviour of the NCC could be recognised. The ice maps were selected at maximum ice extent in the area of the station surveyed in the respective year of the cruise (Cryo-Norwegian Meteorological Institute, 2022).

3.4.1 Distribution within coastal and fjord areas

Figure 14 shows the distribution of the ecotype of all analysed samples with regard to the areas of the catch locations. Cod were found in both coastal and fjord areas. It was discovered that of 24 individuals of Norwegian Coastal cod, 5 were found inside fjords and 19 in coastal areas. Of 37 individuals belonging to Northeast Arctic cod, 22 individuals were located inside fjords and 15 in coastal areas. One hybrid was also found inside a fjord and the remaining 8 in coastal areas.
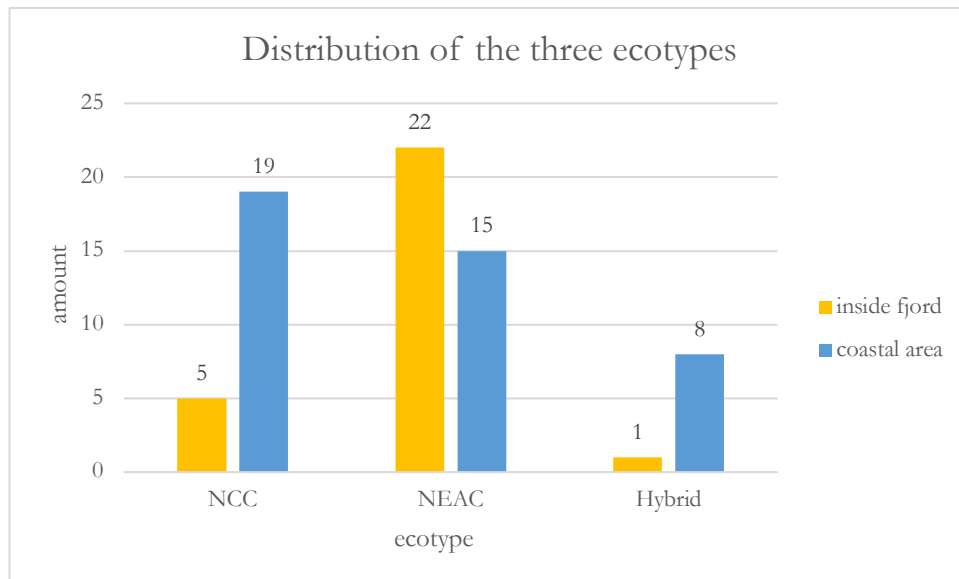
Figure 14: Distribution of Ecotypes.
Ecotype distribution of all analysed samples divided in coastal and fjord areas of Svalbard.

3.4.2 Ecotype distribution in regard of the selected stations

Cod were found at all surveyed stations (Figure 15). It is noticeable that on the west coast (stations 000, 014) most individuals belong to the NCC type of cod. At the two stations in the north of Svalbard (003, 7B) there were more of the NEAC type. At the station near Bear Island, both types of cod are represented equally often. Within the fjords surveyed, most individuals belong to the NEAC ecotype. The group of hybrids is little represented but was found at 6 out of 7 stations.
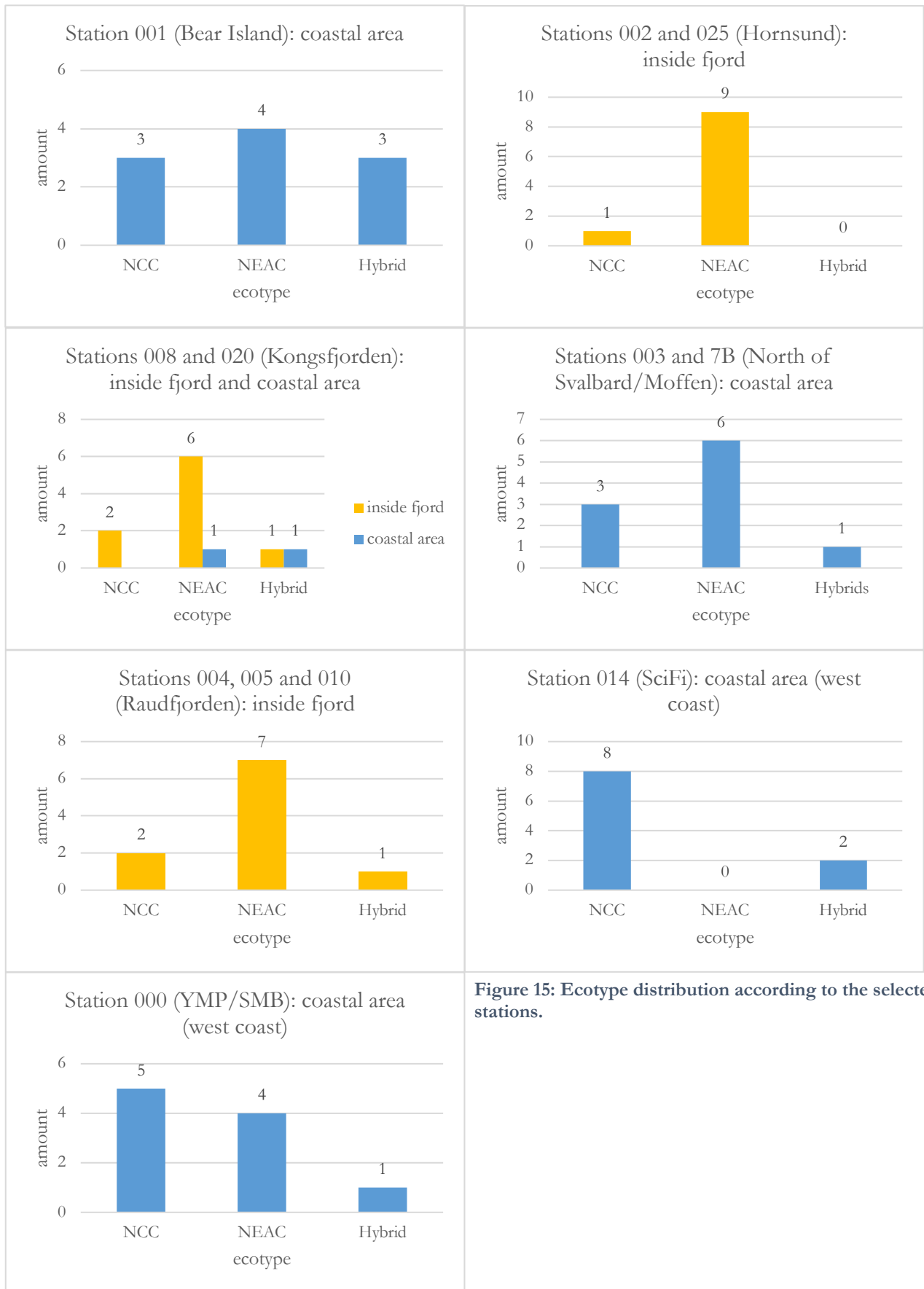
Figure 15: Ecotype distribution according to the selected stations.

3.4.3 Ice cover

When considering the ice maps, it emerged that no area of the stations surveyed was completely covered by ice in 2018. The area around Moffen (003) in the north of Svalbard was freely accessible without drift ice. In Raudfjorden (004, 005), also in the north, the inner part of the fjord was completely covered with ice, but in the front part of the fjord only drift ice was recorded. At the remaining stations on the west coast (002, 008), as well as Bear Island (001), only drift ice was recorded.

In 2020, 3 stations in the north of Svalbard were completely covered with ice (025, 7B, 010). Areas on the west coast of 3 stations (000, 014, 015) were completely ice-free and drift ice was recorded in the area of the remaining station (020).

4   Discussion

The increased warming of the Arctic as consequence of the climate change, may bring a change in Arctic communities. New habitats have opened up due to the decline of sea ice and a northward expansion is possible for species from lower latitudes. One of the species expanding northwards is the Atlantic cod. In this study, it was to investigate whether the Norwegian Coastal cod population can or has established itself in Svalbard. For molecular differentiation of the two cod ecotypes, genotyping using the pantophysin I (Pan I) locus was used.

4.1   Biological consideration

The Pan I locus was used to determine to which ecotype the selected samples for this project belong. It was found that Northeast Arctic cod, Norwegian Coastal cod and hybrids were among 70 tested samples. Among those, 37 individuals were assigned to the NEAC population, 24 to NCC and 9 to the hybrid group. As the NEAC begins its spawning migration south between December and January, NEAC was found in Svalbard during the sampling period between August and October in 2018 and 2020. NEAC is the most frequently represented cod type among the samples in this work, accounting for 53%. This result is consistent with data from other studies, which indicate that the NEAC is the largest known cod stock in the north-east Atlantic and the Barents Sea (Spotowitz et al., 2022). After spawning on the Norwegian west coast, the NEAC undertake their feeding migration towards Svalbard after spawning time from April on and thus also reaches the coasts and fjords of Svalbard in summer.

NCC was also found. 34% of the catch could be assigned to this ecotype. This discovery can be explained by the fact, that the eggs of NCC were passively driven from the spawning grounds in the Lofoten region to Svalbard and due to climate change it can be possible for them to overwinter. The NCC shows less migratory behaviour, only local migrations were attributed to NCC. Therefore, overwintering is dependent on the prevailing conditions on arrival in Svalbard. This study has shown that NCC is present in Svalbard. Accordingly, the offspring must have survived the winter months, if it is assumed that this ecotype is stationary. This means that it is possible for the offspring of NCC to overwinter under the given environmental conditions in Svalbard. The formation of local coastal populations in Svalbard is thus related to the survival during the winter. If the locations of the animals are considered in combination with the ice maps (of the year in which the sampling took place) at maximum ice cover, it can be assumed that there are indeed ice-free areas that are habitable for NCC in winter (7.2, see appendix). In addition, assuming that NCC is a non-migratory cod type, it can be assumed that the NCC found have survive the winters in Svalbard according to their age. More precisely, if an individual has reached its seventh year of life, for example, it can be concluded, that is has already spent seven years in Svalbard. Due to the West

Spitsbergen Current bringing warm Atlantic water along the west coast of Svalbard, this area may be suitable for species coming from lower latitudes to live. This effect is further enhanced by the fact that the temperature of the Atlantic water increases by 0.3°C per decade (Onarheim et al., 2014). This could be the reason why the most frequent appearance of the NCC ecotype at the surveyed stations is on the west coast of Svalbard. In addition, the west coast remains relatively ice-free in winter except for a little drift ice due to the West Spitsbergen Current, offering the chance of wintering in this area. This appearance of the NCC in Svalbard shows the shift of Atlantic species northwards into Arctic waters, enabled by the changing climatic conditions in the Arctic (Lisa Spotowitz et al., 2022).

In addition to the simple fact that NCC has been found, the individuals have reached sizes that are capable of reproduction. Under the mentioned aspect of location fidelity of the NCC in contrast to the NEAC, which migrates back from its feeding ground to its spawning grounds over a long distance every spring, the adults of the NCC in Svalbard must have already survived there for several years, judging by their size. For this purpose, the sizes (TL [cm]) of the animals were assigned to an age class. The results show that the individuals of the NCC found in this study, ranged in size from 19-101 cm, are between 1-11 years old. The individuals of NCC are on average 7 years old with mean length 71,28cm. From point of view of site fidelity, it can be assumed that the animals survived an average 7 years in Svalbard. This allows to investigate the question of whether a local cod population has established itself in Svalbard at the respective sites. The forming of a stock that establishes itself in a new location includes, in addition to survival, the ability to reproduce. According to the literature, coastal cod is capable of reproducing between the ages of five and six years old (Berg & Albert, 2003). Relying on this reference value from the literature, 92% of the analysed animals (figure 8A) may be capable of reproduction, even though it was not examined if NCC found had already spawned. Nevertheless, the two conditions mentioned above for the establishment of a coastal cod stock in Svalbard would be fulfilled. The stage of maturity of the animals was determined during sampling, all individuals were only in stage 1 or 2 (7.1.1, see appendix). Sampling took place at the end of the summer, i.e., about 5-7 months before spawning season beginning in March. Thus, the gonads had already been formed, but they were still maturing. If the sampling had been conducted in the first quarter of the year, the maturity observations, among others, would have been different. But it is possible that, considering that the animals have reached sizes that are reproductive according to the literature, they have found spawning sites in Svalbard and are reproducing there. Furthermore, tagging experiments on coastal cod have shown that they visit the same spawning grounds every year after making only short local migrations (Berg & Albert, 2003). Therefore, it is possible that the found reproductive individuals assigned to the NCC ecotype formed a locally migratory coastal population.

Furthermore, it was decided by using ice maps whether it was possible that the animals spent the last winter at the location where they were found (7.2). If the sampled station was covered with ice last winter, the animals in question could not have spent the winter there. This suggests that the animals migrated to the station of interest in the period between the retreat of the ice cover and the sampling. This discovery of local migrations is consistent with results from a study that also described that NCC undertaking local migrations (Andrade et al., 2020). By looking at the ice maps at the times of maximum ice expansion, specific to the respective stations of the catches, it could be determined that at three out of seven stations it had been impossible for the animals to spend the winter at the location found. The reason for that is, that the ice maps show that in Hornsund (025), Moffen (7B) and Raudfjorden (010), the areas were completely covered by ice in spring during the year of the catch (2020). This confirmed it was unlikely that the animals spent the winter at the stations in question and must have migrated to the site of capture after the sea ice had retreated. It was noticeable that the stations were located in the south and on the north coast of Svalbard. The exact route of the animals could not be determined in this work. Most of the individuals stay on the west coast, which is due to the above-mentioned Atlantic influence in this area. It therefore suggests that the NCC feels most comfortable in this area. The results also show that NEAC also reside along the west coast and north of Svalbard. Thus, it can be concluded that both ecotypes essentially follow the currents of the Gulf Stream. It can therefore be assumed that animals found in the north or south of Svalbard most likely migrate northwards and southwards from this area. This is possible in the period after the maximum ice expansion, which is also the period of the catches. However, in order to create a more specific pattern of NCC migration in Svalbard, a more detailed study has to be performed and more samples have to be collected.

4.2   Methodological consideration

For this study, however, a self-defined range had to be used, since 30 of the 70 samples did not provide clear results. The results from the fragment length analysis are considered unambiguous if either the Pan I allele is homozygous, meaning that only one of the specific primers for the respective allele has bound and thus only one intensity peak is recorded. This intensity peak is at the 77 bp position for Pan I^{BB} or NEAC and at 79 bp for Pan I^{AA} or NCC. Or in the case of heterozygosity, both primers have bound, which means that two peaks of the same intensity should be present at the respective bp positions. Among the results for Pan I^{AA}, however, there are 15 samples in which two peaks were detected for both alleles, whereby the intensity for the Pan I^A allele was clearly stronger. The same was the case for the Pan I^B allele, in which 6 samples were nevertheless classified as homozygous for Pan I^B due to the significantly stronger intensity for the specific primer of the Pan I^B allele than for Pan I^A. In order to be able to assign the ambiguous

samples to a population, ranges (0 to 0,5 Pan I^{BB}, 0,51 to 1,99 Hybrid, off 2,0 Pan I^{AA}) were defined, which allowed a clear classification to the populations. The reasons for the differences in the results compared to those from literature have not yet been conclusively explained. Nevertheless, the results are reproducible because during the phase of optimising the PCR conditions, the same starting DNA was used for different PCR. In the subsequent fragment length analyses, however, the same results were produced for the different PCR products by using identical DNA templates.

5   Summary and Outlook

This project investigated whether a local coastal population of NCC ecotype has formed in Svalbard. For this purpose, the population structure in Svalbard waters was studied. The data survey was carried out in September and October 2018, as well as in August 2020 in the coastal and fjord areas of Svalbard. Tissue samples of muscle and fins, as well as other data such as the total length of the fish were measured. Genotyping of cod from results of fragment length analysis (FLA) after previous allele-specific PCR, was performed using the pantophysin I locus (Pan I). The two ecotypes mentioned can be distinguished by their allelic variants of the Pan I locus. NEAC has the homozygous genotype Pan I^{BB}, whereas NCC is homozygous for the Pan I^A allele. In addition, there is the heterozygous variant Pan I^{AB}, which is assigned to the group of hybrids. Due to a discrepancy in the results from the FLA compared to results from the literature, the data had to be adjusted using a correction factor, as well as a calculated identification factor. It has not yet been sufficiently explained where the origin of these differences lies, although it could be verified and confirmed that the identical initial DNA yields the same divergent FLA results. From the usable and reproducible results, it was found that all three ecotypes of cod occur in Svalbard. It was then investigated whether the cod found assigned to the NCC ecotype had reached sizes that were capable of reproduction, which would allow an answer to the question of whether this type has become established in Svalbard. For this purpose, the individuals were divided into age classes based on their sizes using reference values from the literature. This in turn made it possible to determine whether the animals were already able to reproduce. On the basis of these investigations, it could be shown that the NCC found in Svalbard are in age classes that have been able to spawn for several years. On the basis of the fact that these animals show a stationary behaviour and only undertake local coastal migrations, it can be assumed that they have been in Svalbard for several years. In addition, an investigation of migratory behaviour was carried out using ice maps. The ice maps provide information on whether it was possible for the animals to have survived the last winter at the location where they were caught. At stations on the coast (Moffen, 7B), as well as a fjord (Raudfjorden, 010) in the north of Svalbard and a station in a southern fjord (Hornsund, 025), it could be shown that it was not possible for the animals to have spent the winter at these locations. These areas were completely covered by ice. Since the distribution of the animals in Svalbard shows that most individuals of the NCC were found on the Atlantic-influenced west coast, it can be assumed that the animals undertake southward and northward coastal migrations from there. Tagging experiments on the animals in Svalbard would provide more precise conclusions, which, however, could not be carried out within the context of this work. Finally, the appearance of the NCC, which were on average 7 years old, in Svalbard's coasts and fjord areas shows that it is possible for them to have survived there for several years, assuming site fidelity. With more

profound genetic studies, such as single nucleotide polymorphic (SNP) markers, it would be possible to show more specifically whether the population (NCC) in Svalbard is genetically different from that on the west coast of Norway. Which would support the establishment of a Svalbard Coastal cod (SCC) population. Overall, this finding represents a change in species composition in Svalbard, which may have an effect on the already established Arctic inhabitants there. For this, it would be important that Arctic species in Svalbard are also studied annually to show patterns in any changes.

6 References

Andrade, H., van der Sleen, P., Black, B. A., Godiksen, J. A., Locke, W. L., Carroll, M. L., Ambrose, W. G. & Geffen, A. (2020, 6. April). Ontogenetic movements of cod in Arctic fjords and the Barents Sea as revealed by otolith microchemistry. *Polar Biology*, *43*(5), 409–421. https://doi.org/10.1007/s00300-020-02642-1

Andersen, I., Johnsen, H., De Rosa, M. C., Præbel, K., Stjelja, S., Kirubakaran, T. G., Pirolli, D., Jentoft, S. & Fevolden, S. E. (2015). Evolutionary history and adaptive significance of the polymorphic Pan I in migratory and stationary populations of Atlantic cod (Gadus morhua). *Marine Genomics*, *22*, 45–54. https://doi.org/10.1016/j.margen.2015.03.009

Berg, E. & Albert, O. T. (2003, 1. January). Cod in fjords and coastal waters of North Norway: distribution and variation in length and maturity at age. *ICES Journal of Marine Science*, *60*(4), 787–797. https://doi.org/10.1016/s1054-3139(03)00037-7

Brownstein, M. J., Carpten, J. D. & Smith, J. R. (1996). Modulation of Non-Templated Nucleotide Addition by *Taq*DNA Polymerase: Primer Modifications that Facilitate Genotyping. *BioTechniques*, *20*(6), 1004–1010. https://doi.org/10.2144/96206st01

Cryo - Norwegian Meteorological Institute (2022). Cryo - Norwegian Meteorological Institute. Historical Ice Charts. https://cryo.met.no/en/latest-ice-charts

Dahle, G., Johansen, T., Westgaard, J. I., Aglen, A. & Glover, K. A. (2018). Genetic management of mixed-stock fisheries "real-time": The case of the largest remaining cod fishery operating in the Atlantic in 2007–2017. *Fisheries Research*, *205*, 77–85. https://doi.org/10.1016/j.fishres.2018.04.006

DNeasy Blood & Tissue Handbook - QIAGEN. (o. D.). Abgerufen am 24. September 2022, von https://www.qiagen.com/us/resources/resourcedetail?id=68f29296-5a9f-40fa-8b3d-1c148d0b3030&lang=en

Drinkwater, K. F. (2005, 1. Januar). The response of Atlantic cod (Gadus morhua) to future climate change. *ICES Journal of Marine Science*, *62*(7), 1327–1337. https://doi.org/10.1016/j.icesjms.2005.05.015

Fevolden, S. (2012, 7. Februar). *Brage IMR: Farming of Atlantic cod Gadus morhua in the vicinity of major spawning sites for Norwegian coastal cod populations - is it hazardous?* Havforskningsinstituttet Institute of Marine Research. https://imr.brage.unit.no/imr-xmlui/handle/11250/102994?locale-attribute=en

Fevolden, S. E. & Pogson, G. H. (1997). Genetic divergence at the synaptophysin (Syp I) locus among Norwegian coastal and north-east Arctic populations of Atlantic cod. *Journal of Fish Biology*, *51*(5), 895–908. https://doi.org/10.1111/j.1095-8649.1997.tb01529.x

Haass, N. K., Kartenbeck, M. A. & Leube, R. E. (1996). Pantophysin is a ubiquitously expressed synaptophysin homologue and defines constitutive transport vesicles. *Journal of Cell Biology*, *134*(3), 731–746. https://doi.org/10.1083/jcb.134.3.731

Impacts of climate change on Arctic climate and weather. (o. D.). National Snow and Ice Data Center. Abgerufen am 24. September 2022, von https://nsidc.org/learn/parts-cryosphere/arctic-weather-and-climate/why-arctic-weather-and-climate-matter

Mark, F., Peeken, I., Flores, H., Schauer, U., Soltwedel, T., Storch, D. (2014). The consequences of climate change for life in the Arctic Ocean. Alfred-Wegener-Institut - Fact Sheet. Abgerufen am 28. September 2022, von https://epic.awi.de/id/eprint/46408/1/WEB_UK_Factsheet_ArcticOcean.pdf

Markl, J., Sadava, D., Hillis, D. M., Heller, C. H., Hacker, S. D., Held, A., Jarosch, B., Seidler, L., Niehaus-Osterloh, M., Sixt, E. & Delbrück, M. (2019). *Purves Biologie* (10. Aufl. 2019). Springer Spektrum.

Markusson, H. (2020, 17. April). *Is cod becoming a stationary species in the Svalbard fjords?* Framsenteret. Abgerufen am 24. September 2022, von https://framsenteret.no/nyheter/2020/04/17/is-cod-becoming-a-stationary-species-in-the-svalbard-fjords/

Nordeide, J. T. & Båmstedt, U. (1998, 30. November). Coastal cod and north-east Arctic cod - do they mingle at the spawning grounds in Lofoten? *Sarsia*, *83*(5), 373–379. https://doi.org/10.1080/00364827.1998.10413696

Onarheim, I. H., Smedsrud, L. H., Ingvaldsen, R. B. & Nilsen, F. (2014). Loss of sea ice during winter north of Svalbard. *Tellus A: Dynamic Meteorology and Oceanography*, *66*(1), 23933. https://doi.org/10.3402/tellusa.v66.23933

Otterå, H., Johansen, T., Folkvord, A., Dahle, G., Solvang Bingh, M. K., Westgaard, J. I. & Glover, K. A. (2020). The pantophysin gene and its relationship with survival in early life stages of Atlantic cod. *Royal Society Open Science*, *7*(10), 191983. https://doi.org/10.1098/rsos.191983

Pogson, G. H. (2001). Nucleotide Polymorphism and Natural Selection at the Pantophysin (*Pan* I) Locus in the Atlantic Cod, *Gadus morhua* (L.). *Genetics*, *157*(1), 317–330. https://doi.org/10.1093/genetics/157.1.317

Sarvas, T. H. & Fevolden, S. E. (2005). The scnDNA locus Pan I reveals concurrent presence of different populations of Atlantic cod (Gadus morhua L.) within a single fjord. *Fisheries Research*, *76*(3), 307–316. https://doi.org/10.1016/j.fishres.2005.07.013

Spotowitz, L., Johansen, T., Hansen, A., Berg, E., Stransky, C. & Fischer, P. (2022, 8. September). New evidence for the establishment of coastal cod Gadus morhua in Svalbard fjords. *Marine Ecology Progress Series*, *696*, 119–133. https://doi.org/10.3354/meps14126

Stenvik, J., Wesmajervi, M. S., Damsgard, B. & Delghandi, M. (2006). Genotyping of pantophysin I (Pan I) of Atlantic cod (Gadus morhua L.) by allele-specific PCR. *Molecular Ecology Notes*, *6*(1), 272–275. https://doi.org/10.1111/j.1471-8286.2005.01178.x

Stransky, C., Baumann, H., Fevolden, S. E., Harbitz, A., Høie, H., Nedreaas, K. H., Salberg, A. B. & Skarstein, T. H. (2008, April). Separation of Norwegian coastal cod and Northeast Arctic cod by outer otolith shape analysis. *Fisheries Research*, *90*(1–3), 26–35. https://doi.org/10.1016/j.fishres.2007.09.009

Thermo Fisher Scientific - Site Down. (2009). Microsatellite Analysis Getting Started Guide. https://www.thermofisher.com/nl/en/home/technical-resources/technical-reference-library/capillary-electrophoresis-applications-support-center/fragment-analysis-support.html

Vikebø, F., Sundby, S., Ådlandsvik, B. & Fiksen, Y. (2005). The combined effect of transport and temperature on distribution and growth of larvae and pelagic juveniles of Arcto-Norwegian cod. *ICES Journal of Marine Science*, *62*(7), 1375–1386. https://doi.org/10.1016/j.icesjms.2005.05.017

7 Appendix

7.1 Datafiles

7.1.1 HE519/560 rawdata

smb://smb.isibhv.dmawi.de/winfs/Biowissenschaften/CWithelm/Probentabelle/BA_Probenauswahl.xlsx/BA_HE519_560_rawdata

7.1.2 TL all samples

smb://smb.isibhv.dmawi.de/winfs/Biowissenschaften/CWithelm/Probentabelle/BA_Probenauswahl.xlsx/BA_HE519_560_all_samples_TL

7.1.3 Rawdata FLA

smb://smb.isibhv.dmawi.de/winfs/Biowissenschaften/CWithelm/Auswertung/BA_Auswertung_Datentabelle.xlsx/BA_rawdata_FLA_intensity_bp

7.2 Tables and figures

Table A 1: BA_HE519_560_dataselection.

cruise	date	station_name	station_number	hol	species	id	id_IEP	tissue	TL [cm]	fishing_gear
HE519	28.09.18	Bear Island	001	1	Gadus_morhua	7		F	68,00	fishing rod
HE519	28.09.18	Bear Island	001	1	Gadus_morhua	14		Mu	61,00	fishing rod
HE519	28.09.18	Bear Island	001	2	Gadus_morhua	16		F	101,00	bottom trawl
HE519	28.09.18	Bear Island	001	3	Gadus_morhua	20		F	80,00	bottom trawl
HE519	28.09.18	Bear Island	001	3	Gadus_morhua	21		F	87,00	bottom trawl
HE519	28.09.18	Bear Island	001	3	Gadus_morhua	23		F	53,00	bottom trawl
HE519	28.09.18	Bear Island	001	3	Gadus_morhua	24		F	52,00	bottom trawl
HE519	28.09.18	Bear Island	001	3	Gadus_morhua	35		Mu	55,00	bottom trawl
HE519	28.09.18	Bear Island	001	3	Gadus_morhua	36		Mu	59,00	bottom trawl

Cruise	Date	Location	Station	Group	Species	No.	Count	Sex	Length	Method
HE519	28.09.18	Bear Island	001	3	Gadus_morhua	50		F	46,00	bottom trawl
HE519	29.09.18	Hornsund	002	5	Gadus_morhua	67		Mu	54,00	fish lift
HE519	29.09.18	Hornsund	002	5	Gadus_morhua	69		F	17,50	fish lift
HE519	29.09.18	Hornsund	002	5	Gadus_morhua	73		F	19,00	fish lift
HE519	29.09.18	Hornsund	002	5	Gadus_morhua	79		F	21,00	fish lift
HE519	29.09.18	Hornsund	002	5	Gadus_morhua	84		F	18,00	fish lift
HE519	29.09.18	Hornsund	002	5	Gadus_morhua	90		F	19,50	fish lift
HE519	29.09.18	Hornsund	002	5	Gadus_morhua	93		F	13,00	fish lift
HE519	29.09.18	Hornsund	002	5	Gadus_morhua	94		F	20,00	fish lift
HE560	30.08.20	Hornsund	025		Gadus_morhua		1450	F	61	fishing rod
HE560	30.08.20	Hornsund	025		Gadus_morhua		1460	F	35	fishing rod
HE519	03.10.18	Kongsfjorden	008	5A	Gadus_morhua	232		Mu	65,00	fishing rod
HE519	03.10.18	Kongsfjorden	008	5A	Gadus_morhua	235		F	49,00	fishing rod
HE519	03.10.18	Kongsfjorden	008	5A	Gadus_morhua	239		F	71,00	fishing rod
HE519	03.10.18	Kongsfjorden	008	5A	Gadus_morhua	241		Mu	59,00	fishing rod
HE519	03.10.18	Kongsfjorden	008	5A	Gadus_morhua	255		F	54,00	fishing rod
HE519	03.10.18	Kongsfjorden	008	5A	Gadus_morhua	265		F	80,00	fishing rod
HE519	03.10.18	Kongsfjorden	008	5A	Gadus_morhua	280		Mu	101,00	fishing rod
HE519	03.10.18	Kongsfjorden	008	5A	Gadus_morhua	284		Mu	46,00	fishing rod
HE560	25.08.20	Kongsfjorden	020	1	Gadus_morhua		1135	F	94	bottom trawl
HE560	21.08.20	Kongsfjorden 2	015	8	Gadus_morhua		1202	F	40	bottom trawl
HE519	30.09.18	Moffen	003	4	Gadus_morhua	98		F	42,00	fishing rod
HE519	30.09.18	Moffen	003	4	Gadus_morhua	102		Mu	46,00	fishing rod
HE519	30.09.18	Moffen	003	4	Gadus_morhua	109		Mu	49,00	fishing rod
HE519	30.09.18	Moffen	003	4	Gadus_morhua	115		Mu	78,00	fishing rod
HE519	30.09.18	Moffen	003	4	Gadus_morhua	116		Mu	75,00	fishing rod
HE560	14.08.20	Moffen	7B		Gadus_morhua		441	F	58	fishing rod
HE560	14.08.20	Moffen	7B		Gadus_morhua		382	F	36	fishing rod
HE560	14.08.20	Moffen	7B		Gadus_morhua		803	F	28	fishing rod
HE560	14.08.20	Moffen	7B		Gadus_morhua		798	F	32	fishing rod

HE560	14.08.20	Moffen	7B	3	Gadus_morhua		836	F	24	fishing rod
HE519	01.10.18	Raudfjorden	004	3	Gadus_morhua	123		Mu	59,00	fish lift
HE519	01.10.18	Raudfjorden	004	3	Gadus_morhua	125		Mu	37,00	fish lift
HE519	01.10.18	Raudfjorden	004	3	Gadus_morhua	127		Mu	67,00	fish lift
HE519	01.10.18	Raudfjorden	004	3	Gadus_morhua	122		Mu	78,00	fish lift
HE519	17.08.20	Raudfjorden	010	7	Gadus_morhua		763	F	89	fish lift
HE560	17.08.20	Raudfjorden	010	7	Gadus_morhua		722	F	56	fish lift
HE560	17.08.20	Raudfjorden	010	7	Gadus_morhua		731	F	63	fish lift
HE519	01.10.18	Raudfjorden	005	1	Gadus_morhua	130		F	49,00	fish lift
HE519	01.10.18	Raudfjorden	005	1	Gadus_morhua	131		F	70,00	fish lift
HE519	01.10.18	Raudjorden	005	1	Gadus_morhua	138		F	81,00	fish lift
HE560	20.08.20	SciFi	014		Gadus_morhua		1184	F	84	fishing rod
HE560	20.08.20	SciFi	014		Gadus_morhua		1302	F	96	fishing rod
HE560	20.08.20	SciFi	014		Gadus_morhua		1087	F	77	fishing rod
HE519	20.08.20	SciFi	014		Gadus_morhua		1161	F	60	fishing rod
HE519	20.08.20	SciFi	014		Gadus_morhua		1117	F	59	fishing rod
HE519	20.08.20	SciFi	014		Gadus_morhua		1180	F	72	fishing rod
HE560	20.08.20	SciFi	014		Gadus_morhua		1229	F	67	fishing rod
HE560	20.08.20	SciFi	014		Gadus_morhua		1125	F	89	fishing rod
HE560	20.08.20	SciFi	014		Gadus_morhua		1301	F	78	fishing rod
HE560	20.08.20	SciFi	014		Gadus_morhua		1215	F	74	fishing rod
HE560	20.08.20	SciFi	014		Gadus_morhua		137	F	72	fishing rod
HE560	09.08.20	YMP / SMB	000		Gadus_morhua		70	F	87	fishing rod
HE560	09.08.20	YMP / SMB	000		Gadus_morhua		154	F	57	fishing rod
HE560	09.08.20	YMP / SMB	000		Gadus_morhua		191	F	94	fishing rod
HE560	09.08.20	YMP / SMB	000		Gadus_morhua		28	F	81	fishing rod
HE560	09.08.20	YMP / SMB	000		Gadus_morhua		143	F	110	fishing rod
HE560	09.08.20	YMP / SMB	000		Gadus_morhua		186	F	53	fishing rod
HE560	09.08.20	YMP / SMB	000		Gadus_morhua		91	F	60	fishing rod
HE560	09.08.20	YMP / SMB	000		Gadus_morhua		52	F	67	fishing rod

HE560	09.08.20	YMP / SMB	000		Gadus_morhua		171	F	78	fishing rod

Table A 2: DNA concentrations (ng/µl).

Sample ID	Date	Time	ng/ul	A260	A280	260/280
GmoH025	20.01.22	15:03	138,15	2,763	1,238	2,23
GmoH026	20.01.22	15:04	145,27	2,905	1,349	2,15
GmoH027	20.01.22	15:05	53,96	1,079	0,508	2,13
GmoH028	20.01.22	15:06	214,38	4,288	1,979	2,17
GmoH029	20.01.22	15:07	194,6	3,892	1,785	2,18
GmoH030	20.01.22	15:08	347,13	6,943	3,166	2,19
GmoH031	02.03.22	08:33	243,79	4,876	2,265	2,15
GmoH033	02.03.22	08:36	100,36	2,007	0,916	2,19
GmoH035	02.03.22	08:38	85,4	1,708	0,761	2,25
GmoH037	02.03.22	08:40	112,59	2,252	1,004	2,24
GmoH040	02.03.22	08:43	108,06	2,161	0,963	2,24
GmoH041	02.03.22	08:44	73,67	1,473	0,673	2,19
GmoH042	15.03.22	09:43	112,77	2,255	1,026	2,2
GmoH043	15.03.22	09:45	110,68	2,214	1,015	2,18
GmoH044	15.03.22	09:46	20,36	0,407	0,187	2,17
GmoH047	15.03.22	09:50	86,12	1,722	0,782	2,2
GmoH046	15.03.22	09:51	87,59	1,752	0,779	2,25
GmoH045	15.03.22	09:52	83,76	1,675	0,773	2,17
GmoH048	15.03.22	09:53	63,42	1,268	0,561	2,26
GmoH049	15.03.22	09:55	83,57	1,671	0,909	1,84
GmoH050	15.03.22	09:56	95,04	1,901	0,877	2,17
GmoH051	15.03.22	09:58	53,35	1,067	0,492	2,17
GmoH052	15.03.22	09:59	250,9	5,018	2,272	2,21
GmoH053	15.03.22	10:00	130,43	2,609	1,172	2,23
GmoH054	15.03.22	10:01	99,62	1,992	0,912	2,18
GmoH055	15.03.22	10:02	117,14	2,343	1,079	2,17
GmoH056	15.03.22	10:03	116,21	2,324	1,058	2,2
GmoH057	15.03.22	10:04	146,6	2,932	1,328	2,21

GmoH058	15.03.22	10:05	153,14	3,063	1,398	2,19
GmoH059	15.03.22	10:06	114,99	2,3	1,05	2,19
GmoH060	15.03.22	10:07	142,9	2,858	1,311	2,18
GmoH061	15.03.22	10:08	171,6	3,432	1,566	2,19
GmoH062	15.03.22	10:09	70,05	1,401	0,624	2,25
GmoH063	15.03.22	10:10	101,06	2,021	0,922	2,19
GmoH064	15.03.22	10:11	82,84	1,657	0,736	2,25
GmoH065	15.03.22	10:12	128,08	2,562	1,149	2,23
GmoH066	15.03.22	10:14	150,99	3,02	1,371	2,2
GmoH067	15.03.22	10:14	132,41	2,648	1,18	2,24
GmoH068	15.03.22	10:15	97,32	1,946	0,857	2,27
GmoH069	15.03.22	10:16	301,61	6,032	2,745	2,2
GmoH070	15.03.22	10:17	245,53	4,911	2,204	2,23
GmoH071	15.03.22	10:18	270,65	5,413	2,418	2,24
GmoH072	15.03.22	10:19	246,23	4,925	2,19	2,25
GmoH073	15.03.22	10:20	329,23	6,585	2,96	2,22
GmoH074	15.03.22	10:21	272,44	5,449	2,474	2,2
GmoH075	15.03.22	10:22	122,95	2,459	1,089	2,26
GmoH076	15.03.22	10:23	100,26	2,005	0,904	2,22
GmoH077	15.03.22	10:31	21,54	0,431	0,174	2,48
GmoH078	15.03.22	10:32	212,4	4,248	1,971	2,16
GmoH079	15.03.22	10:34	65,52	1,31	0,605	2,17
GmoH080	15.03.22	10:35	45,43	0,909	0,43	2,12
GmoH081	15.03.22	10:36	50,03	1,001	0,452	2,21
GmoH082	15.03.22	10:37	126,65	2,533	1,126	2,25
GmoH083	15.03.22	10:38	91,78	1,836	0,818	2,24
GmoH084	15.03.22	10:39	149,25	2,985	1,353	2,21
GmoH085	15.03.22	10:40	75,76	1,515	0,688	2,2
GmoH086	15.03.22	10:41	117,45	2,349	1,051	2,23
GmoH087	15.03.22	10:42	135	2,7	1,318	2,05

GmoH088	15.03.22	10:43	131,58	2,632	1,19	2,21
GmoH089	15.03.22	10:44	105,15	2,103	0,976	2,16
GmoH090	15.03.22	10:45	66,03	1,321	0,59	2,24
GmoH091	15.03.22	10:46	305,94	6,119	2,787	2,2
GmoH092	15.03.22	10:47	192,67	3,853	1,748	2,2
GmoH093	15.03.22	10:48	317,03	6,341	2,895	2,19
GmoH094	15.03.22	10:49	289,59	5,792	2,643	2,19
GmoH095	15.03.22	10:50	361,84	7,237	3,355	2,16
GmoH096	15.03.22	10:51	225,85	4,517	2,095	2,16
GmoH097	15.03.22	10:51	235,35	4,707	2,166	2,17
GmoH098	15.03.22	10:52	343,84	6,877	3,209	2,14
GmoH099	15.03.22	10:53	464,07	9,281	4,342	2,14

Table A 3: Correction of the intensity of Pan I^A using corr$_f$

GmoHxxx	ROX75	Pan I^A	corr$_f$	Rox75$_{corr}$	Pan I$^A_{corr}$	Pan I$^A_{corr}$
GmoH025	844	642	0,592417062	500	380,3317536	380
GmoH026	1133	543	0,441306267	500	239,6293027	240
GmoH027	858	52	0,582750583	500	30,3030303	30
GmoH028	604	2510	0,82781457	500	2077,81457	2078
GmoH029	560	0	0,892857143	500	0	0
GmoH030	457	0	1,094091904	500	0	0
GmoH031	1112	117	0,449640288	500	52,60791367	53
GmoH033	726	0	0,688705234	500	0	0
GmoH035	571	0	0,875665743	500	0	0
GmoH037	645	65	0,775193798	500	50,3875969	50
GmoH040	761	0	0,657030223	500	0	0
GmoH041	688	1221	0,726744186	500	887,3546512	887
GmoH042	1138	603	0,439367311	500	264,9384886	265
GmoH043	779	782	0,641848524	500	501,9255456	502
GmoH044	494	1446	1,012145749	500	1463,562753	1464
GmoH045	452	0	1,10619469	500	0	0
GmoH046	497	345	1,006036217	500	347,082495	347
GmoH047	510	0	0,980392157	500	0	0
GmoH048	432	101	1,157407407	500	116,8981481	117
GmoH049	528	205	0,946969697	500	194,1287879	194
GmoH050	894	0	0,559284116	500	0	0
GmoH051	620	565	0,806451613	500	455,6451613	456
GmoH052	535	0	0,934579439	500	0	0
GmoH053	407	844	1,228501229	500	1036,855037	1037
GmoH054	371	0	1,347708895	500	0	0
GmoH055	473	1276	1,057082452	500	1348,837209	1349
GmoH056	526	1675	0,950570342	500	1592,205323	1592
GmoH057	703	0	0,711237553	500	0	0

GmoH058	1122	1309	0,445632799	500	583,3333333	583
GmoH059	821	0	0,609013398	500	0	0
GmoH060	521	0	0,95692898	500	0	0
GmoH061	459	1814	1,089324619	500	1976,034858	1976
GmoH062	504	298	0,992063492	500	295,6349206	296
GmoH063	555	331	0,900900901	500	298,1981982	298
GmoH064	462	441	1,082251082	500	477,2727273	477
GmoH065	532	310	0,939849624	500	291,3533835	291
GmoH066	945	0	0,529100529	500	0	0
GmoH067	626	347	0,798722045	500	277,1565495	277
GmoH068	446	908	1,121076233	500	1017,93722	1018
GmoH069	447	0	1,118568233	500	0	0
GmoH070	398	146	1,256281407	500	183,4170854	183
GmoH071	499	0	1,00200408	500	0	0
GmoH072	416	0	1,201923077	500	0	0
GmoH073	474	0	1,054852321	500	0	0
GmoH074	945	0	0,529100529	500	0	0
GmoH075	623	0	0,802568218	500	0	0
GmoH076	558	0	0,896057348	500	0	0
GmoH077	415	707	1,204819277	500	851,8072289	852
GmoH078	388	0	1,288659794	500	0	0
GmoH079	490	542	1,020408163	500	553,0612245	553
GmoH080	551	176	0,907441016	500	159,7096189	160
GmoH081	681	0	0,734214391	500	0	0
GmoH082	1116	0	0,448028674	500	0	0
GmoH083	857	752	0,583430572	500	438,73979	439
GmoH084	576	0	0,868055556	500	0	0
GmoH085	469	0	1,066098081	500	0	0
GmoH086	483	0	1,035196687	500	0	0
GmoH087	548	0	0,912408759	500	0	0

	ROX75	Pan I$_B$	corr$_f$	ROX75$_{corr}$	Pan I$_{Bcorr}$	Pan I$_{Bcorr}$
GmoH088	505	0	0,99009901	500	0	0
GmoH089	563	0	0,88809467	500	0	0
GmoH090	936	0	0,534188034	500	0	0
GmoH091	667	1064	0,74925187	500	797,6011994	798
GmoH092	631	1446	0,792393027	500	1145,800317	1146
GmoH093	464	1494	1,077586207	500	1609,913793	1610
GmoH094	447	1327	1,118568233	500	1484,340045	1484
GmoH095	561	2785	0,891265597	500	2482,174688	2482
GmoH096	573	3416	0,872600349	500	2980,802792	2981
GmoH097	737	2292	0,678426052	500	1554,95251	1555
GmoH098	434	4076	1,152073733	500	4695,852535	4696
GmoH099	420	2198	1,19047619	500	2616,666667	2617

Table A 4: Correction of the intensity of Pan I$_B$ using corr$_f$.

GmoHxxx	ROX75	Pan I$_B$	corr$_f$	ROX75$_{corr}$	Pan I$_{Bcorr}$	Pan I$_{Bcorr}$
GmoH025	675	1139	0,740740741	500	843,7037037	844
GmoH026	519	300	0,963391137	500	289,017341	289
GmoH027	562	746	0,889679715	500	663,7010676	664
GmoH028	679	459	0,736377025	500	337,9970545	338
GmoH029	453	17568	1,103752759	500	19390,72848	19391
GmoH030	523	1162	0,956022945	500	1110,898662	1111
GmoH031	529	938	0,945179584	500	886,5784499	887
GmoH033	761	312	0,657030223	500	204,9934297	205
GmoH035	1303	319	0,383729854	500	122,4098235	122
GmoH037	801	287	0,624219725	500	179,1510612	179
GmoH040	723	754	0,691562932	500	521,4384509	521
GmoH041	749	329	0,667556742	500	219,6261682	220

GmoH042	1163	323	0,42992922614	500	138,8650043	139
GmoH043	841	501	0,594530321	500	297,8596908	298
GmoH044	507	540	0,986193294	500	532,5443787	533
GmoH045	484	713	1,033057851	500	736,5702479	737
GmoH046	521	130	0,959692898	500	124,7600768	125
GmoH047	564	130	0,886524823	500	115,248227	115
GmoH048	465	0	1,075268817	500	0	0
GmoH049	553	156	0,904159132	500	141,0488246	141
GmoH050	964	984	0,518672199	500	510,373444	510
GmoH051	606	104	0,825082508	500	85,80858086	86
GmoH052	582	61	0,859106529	500	52,40549828	52
GmoH053	426	222	1,17370892	500	260,5633803	261
GmoH054	416	377	1,201923077	500	453,125	453
GmoH055	512	413	0,9765625	500	403,3203125	403
GmoH056	560	0	0,892857143	500	0	0
GmoH057	750	1227	0,666666667	500	818	818
GmoH058	1132	944	0,441696113	500	416,9611307	417
GmoH059	816	882	0,612745098	500	540,4411765	540
GmoH060	525	754	0,952380952	500	718,0952381	718
GmoH061	473	0	1,057082452	500	0	0
GmoH062	531	114	0,941619586	500	107,3446328	107
GmoH063	538	98	0,929368803	500	91,07806691	91
GmoH064	469	879	1,066098081	500	937,1002132	937
GmoH065	540	0	0,925925926	500	0	0
GmoH066	958	1631	0,521920668	500	851,2526096	851
GmoH067	612	263	0,816993464	500	214,869281	215
GmoH068	563	399	0,888099467	500	354,3516874	354

GmoH069	438	105	1,141552511	500	119,8630137	120
GmoH070	427	71	1,170960187	500	83,1381733	83
GmoH071	593	63	0,84317032	500	53,11973019	53
GmoH072	489	58	1,022494888	500	59,30470348	59
GmoH073	556	56	0,89928576	500	50,35971223	50
GmoH074	946	597	0,528541226	500	315,5391121	316
GmoH075	671	299	0,745156483	500	222,8017884	223
GmoH076	610	668	0,819672131	500	547,5409836	548
GmoH077	472	136	1,059322034	500	144,0677966	144
GmoH078	454	670	1,101321586	500	737,8854626	738
GmoH079	545	171	0,917431193	500	156,8807339	157
GmoH080	607	826	0,823723229	500	680,3953871	680
GmoH081	737	980	0,678426052	500	664,8575305	665
GmoH082	1139	2042	0,438981563	500	896,4003512	896
GmoH083	879	339	0,568828214	500	192,8327645	193
GmoH084	580	912	0,862068966	500	786,2068966	786
GmoH085	454	549	1,101321586	500	604,6255507	605
GmoH086	521	459	0,959692898	500	440,4990403	440
GmoH087	580	522	0,862068966	500	450	450
GmoH088	534	474	0,936329588	500	443,8202247	444
GmoH089	581	674	0,860585198	500	580,0344234	580
GmoH090	925	1414	0,540540541	500	764,3243243	764
GmoH091	657	587	0,761035008	500	446,7275495	447
GmoH092	597	0	0,837520938	500	0	0
GmoH093	482	0	1,037344398	500	0	0
GmoH094	448	0	1,116071429	500	0	0
GmoH095	561	365	0,891265597	500	325,311943	325

GmoHxxx						
GmoH096	584	0	0,85164384	500	0	0
GmoH097	764	1338	0,654450262	500	875,6544503	876
GmoH098	445	0	1,123595506	500	0	0
GmoH099	550	381	0,909090909	500	346,3636364	346

Table A 5: Calculation of ident_f.

GmoHxxx	Pan I$^A_{corr}$	Pan I$^B_{corr}$	ident$_f$
GmoH025	380	844	0,45
GmoH026	240	289	0,83
GmoH027	30	664	0,05
GmoH028	2078	338	6,15
GmoH029	0	19391	0,00
GmoH030	0	1111	0,00
GmoH031	53	887	0,06
GmoH033	0	205	0,00
GmoH035	0	122	0,00
GmoH037	50	179	0,28
GmoH040	0	521	0,00
GmoH041	887	220	4,04
GmoH042	265	139	1,91
GmoH043	502	298	1,69
GmoH044	1464	533	2,75

GmoHxxx	Pan I$^A_{corr}$	Pan I$^B_{corr}$	ident$_f$
GmoH065	291	0	>2,0
GmoH066	0	851	0,00
GmoH067	277	215	1,29
GmoH068	1018	354	2,87
GmoH069	0	120	0,00
GmoH070	183	83	2,21
GmoH071	0	53	0,00
GmoH072	0	59	0,00
GmoH073	0	50	0,00
GmoH074	0	316	0,00
GmoH075	0	223	0,00
GmoH076	0	548	0,00
GmoH077	852	144	5,91
GmoH078	0	738	0,00
GmoH079	553	157	3,53

GmoH045	0	737	0,00
GmoH046	347	125	2,78
GmoH047	0	115	0,00
GmoH048	117	0	>2,0
GmoH049	194	141	1,38
GmoH050	0	510	0,00
GmoH051	456	86	5,31
GmoH052	0	52	0,00
GmoH053	1037	261	3,98
GmoH054	0	453	0,00
GmoH055	1349	403	3,34
GmoH056	1592	0	>2,0
GmoH057	0	818	0,00
GmoH058	583	417	1,40
GmoH059	0	540	0,00
GmoH060	0	718	0,00
GmoH061	1976	0	>2,0
GmoH062	296	107	2,75
GmoH063	298	91	3,27
GmoH064	477	937	0,51

GmoH080	160	680	0,23
GmoH081	0	665	0,00
GmoH082	0	896	0,00
GmoH083	439	193	2,28
GmoH084	0	786	0,00
GmoH085	0	605	0,00
GmoH086	0	440	0,00
GmoH087	0	450	0,00
GmoH088	0	444	0,00
GmoH089	0	580	0,00
GmoH090	0	764	0,00
GmoH091	798	447	1,79
GmoH092	1146	0	>2,0
GmoH093	1610	0	>2,0
GmoH094	1484	0	>2,0
GmoH095	2482	325	7,63
GmoH096	2981	0	>2,0
GmoH097	1555	876	1,78
GmoH098	4696	0	>2,0
GmoH099	2617	346	7,55
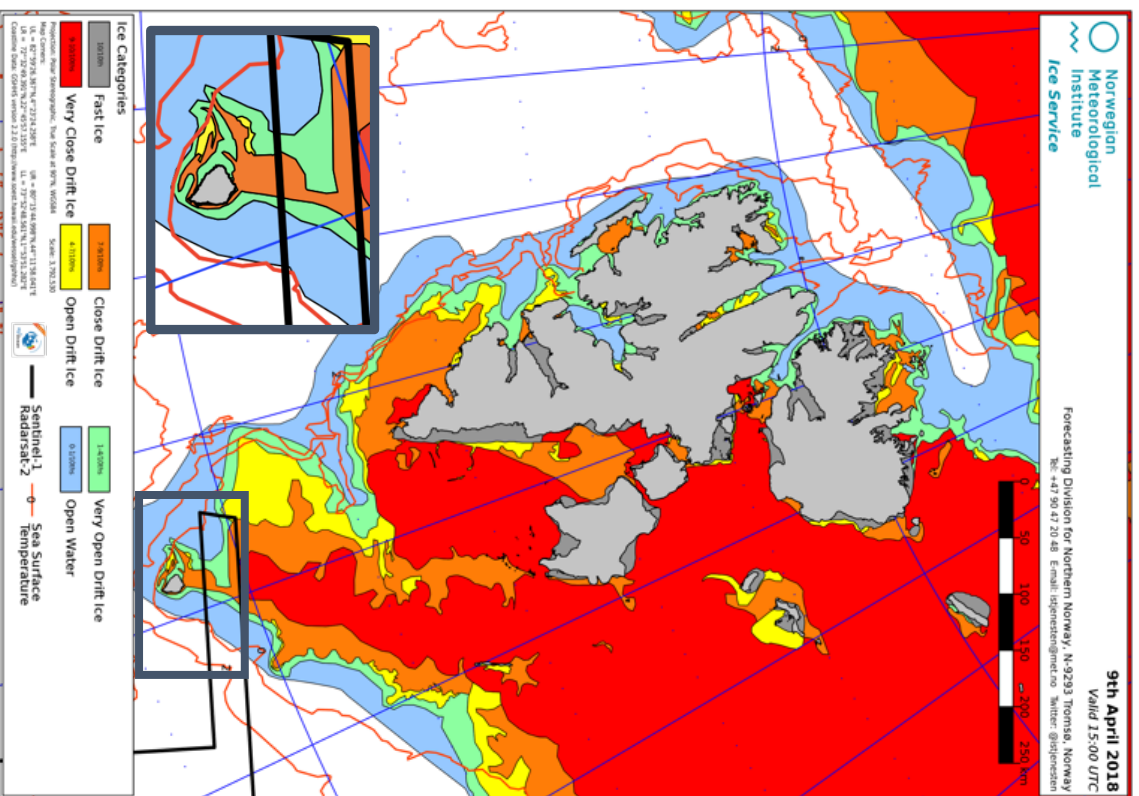
Figure A 1: Ice map Svalbard 9th April 2018. Bear Island 001 (grey framed).
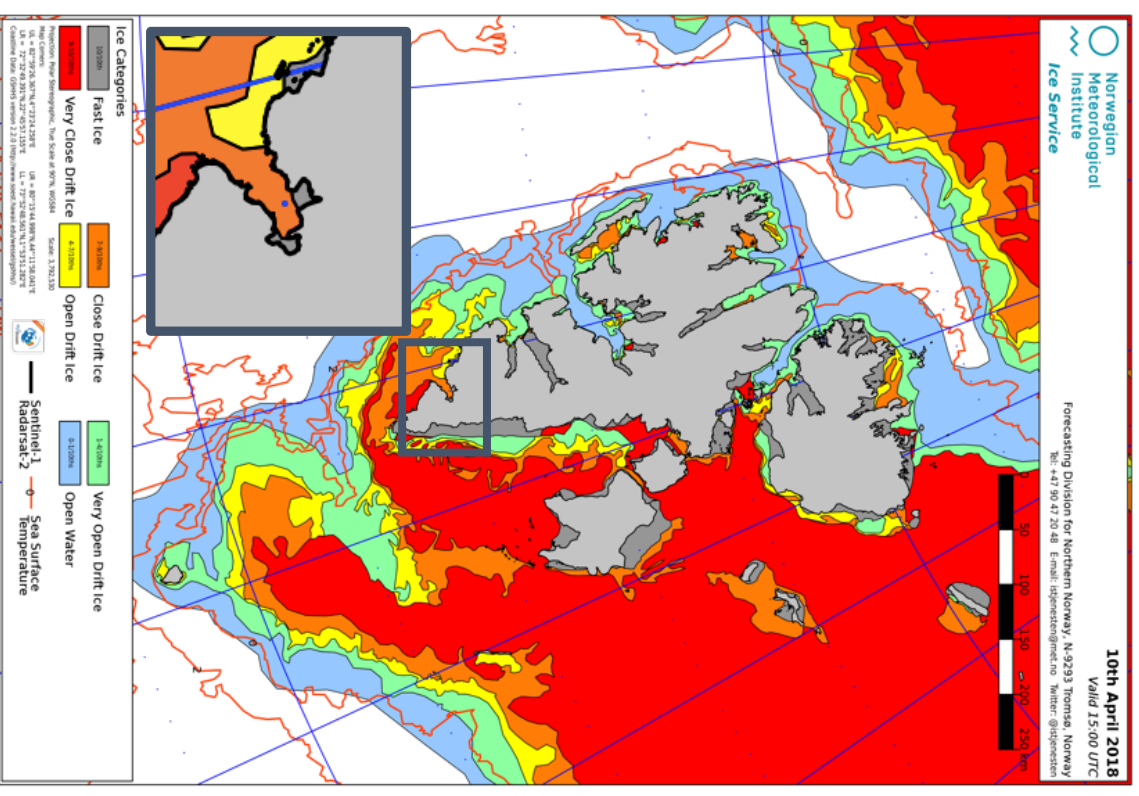
Figure A 2: Ice map Svalbard 10th April 2018. Hornsund 002 (grey framed).
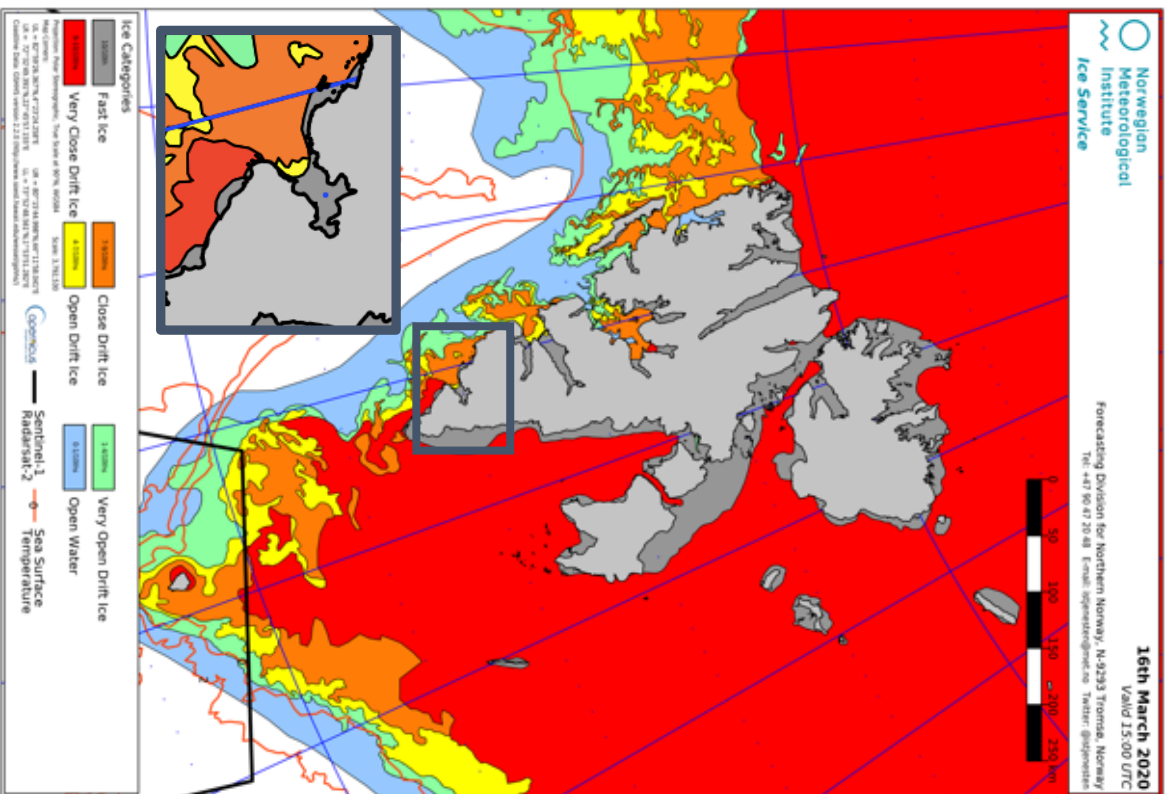
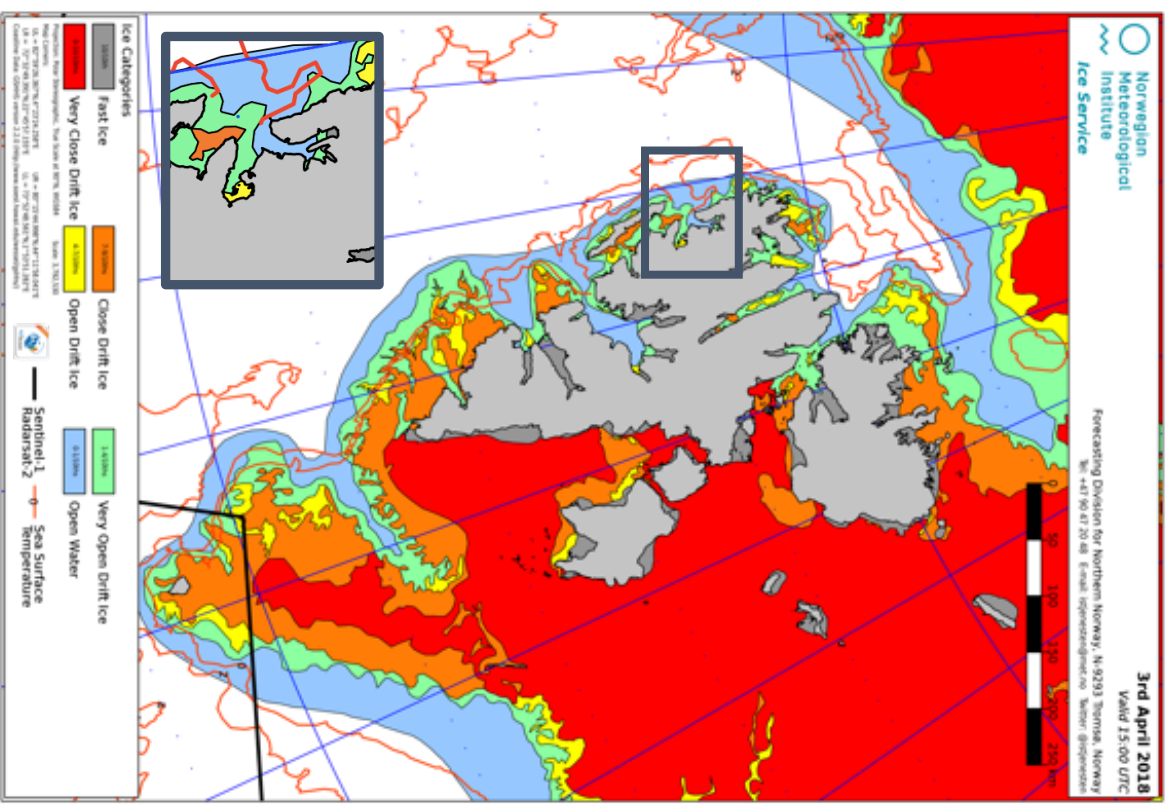Figure A 3: Ice map Svalbard 16th March 2020. Hornsund 025 (grey framed).

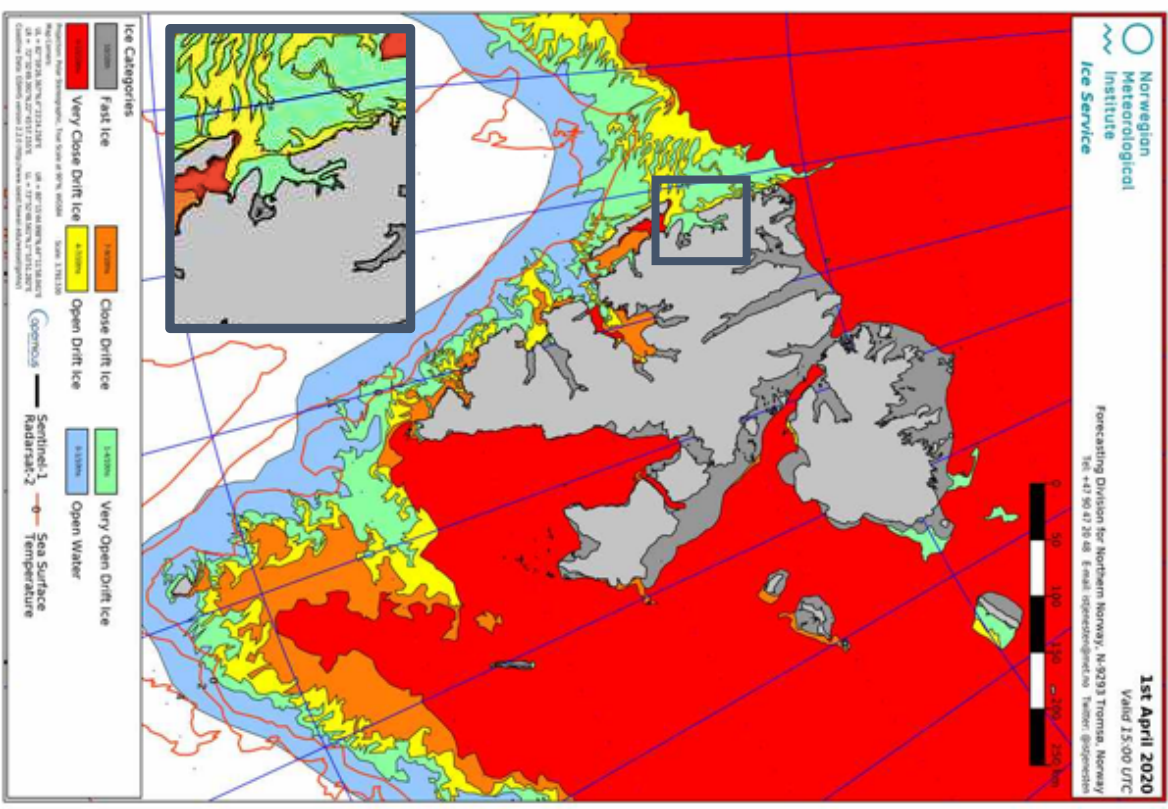Figure A 4: Ice Map Svalbard 3rd April 2018. Kongsfjorden 008 (grey framed).

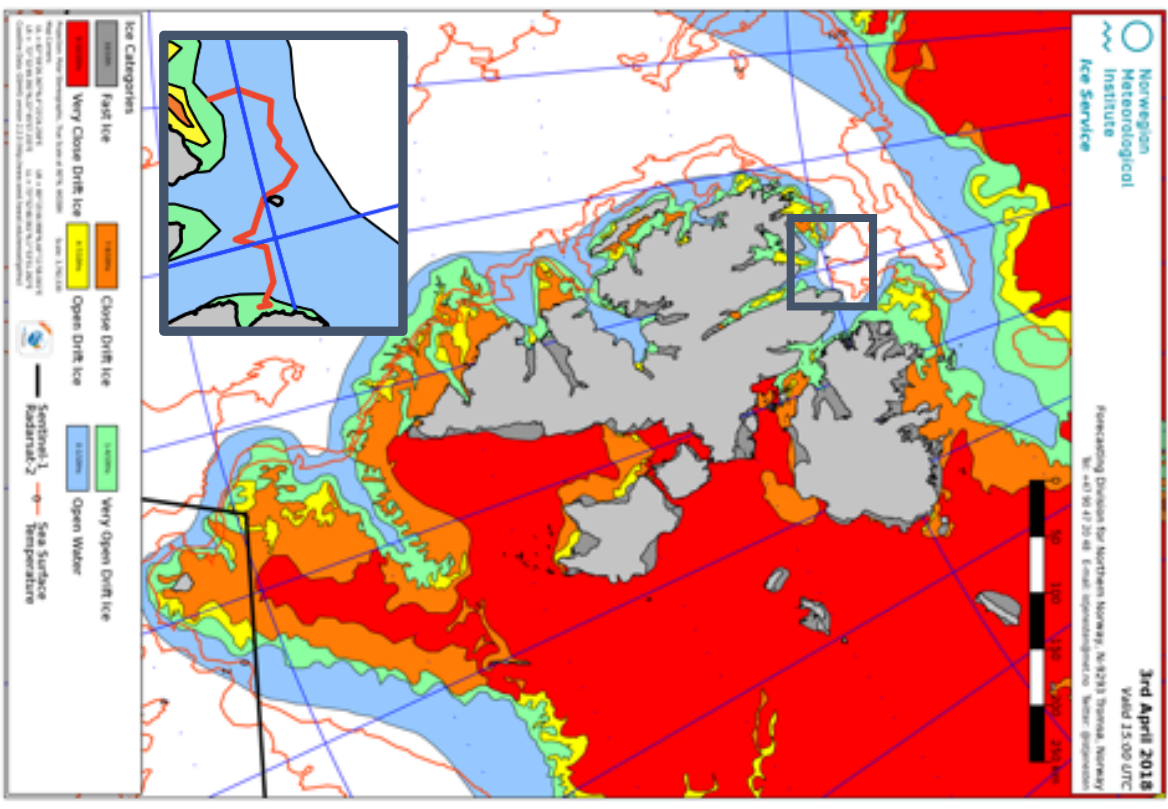Figure A 6: Ice Map Svalbard 1st April 2020. Kongsfjorden 020 (grey framed).

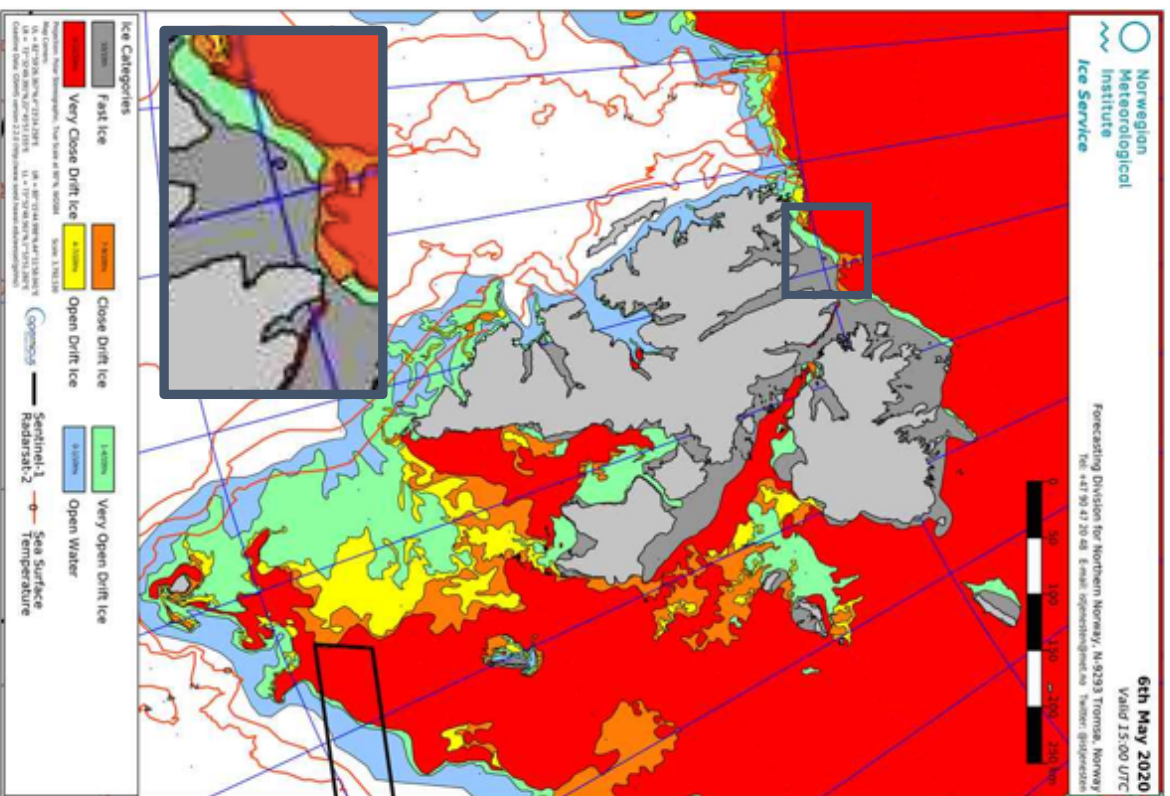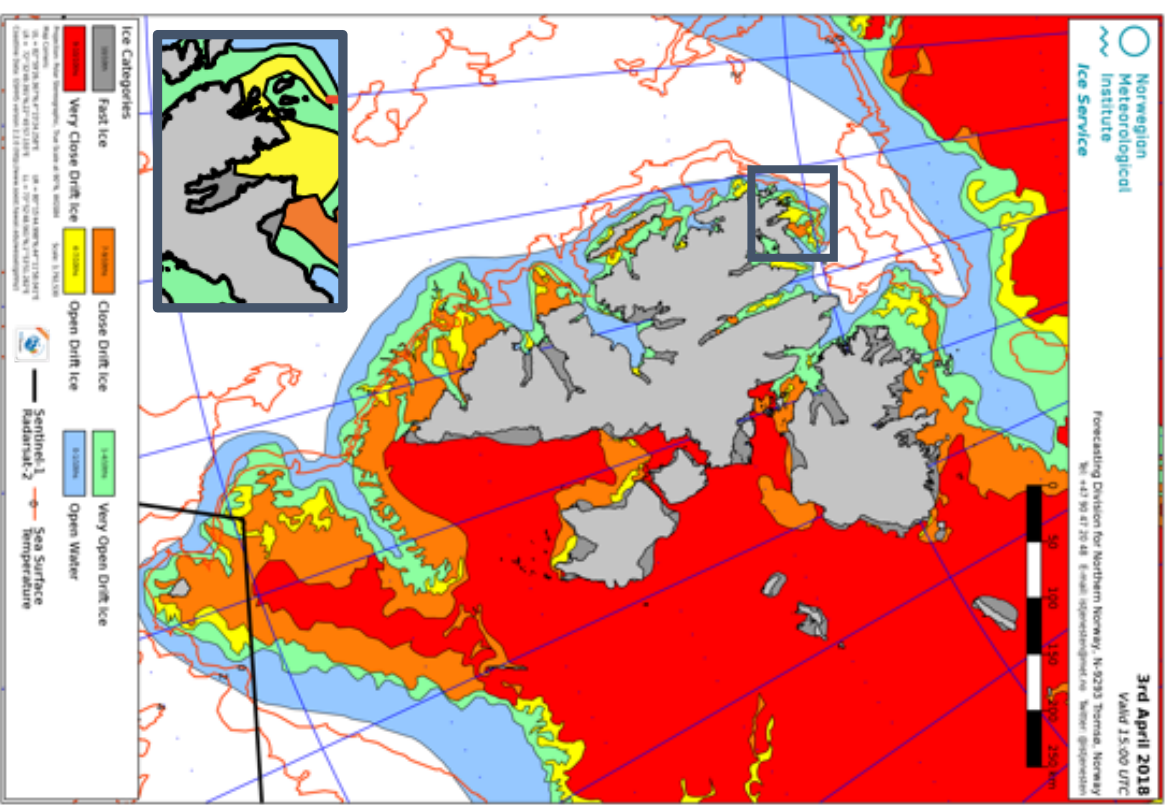Figure A 5: Ice map Svalbard 3rd April 2018. Moffen 003 (grey framed).

Figure A 7 Ice map Svalbard 6th May 2020. Moffen 7B (grey framed).

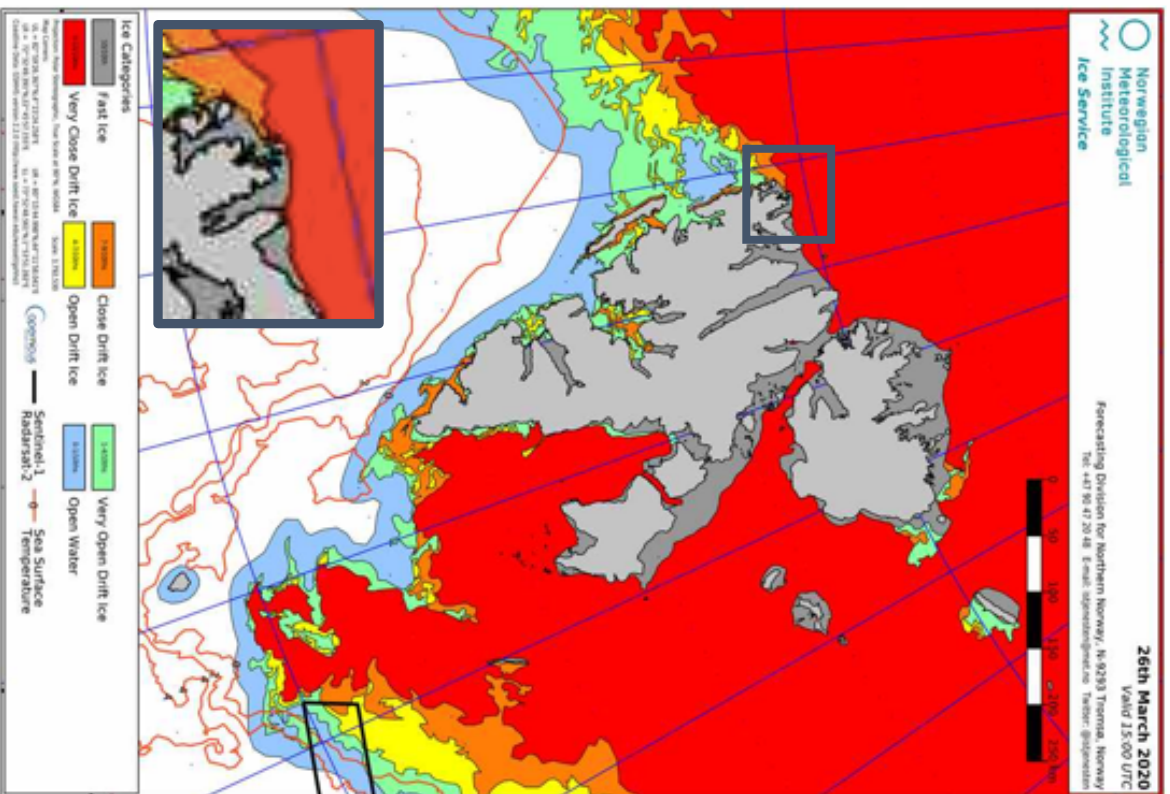Figure A 8: Ice map Svalbard 3rd April 2018. Raudfjorden 004/005 (grey framed).

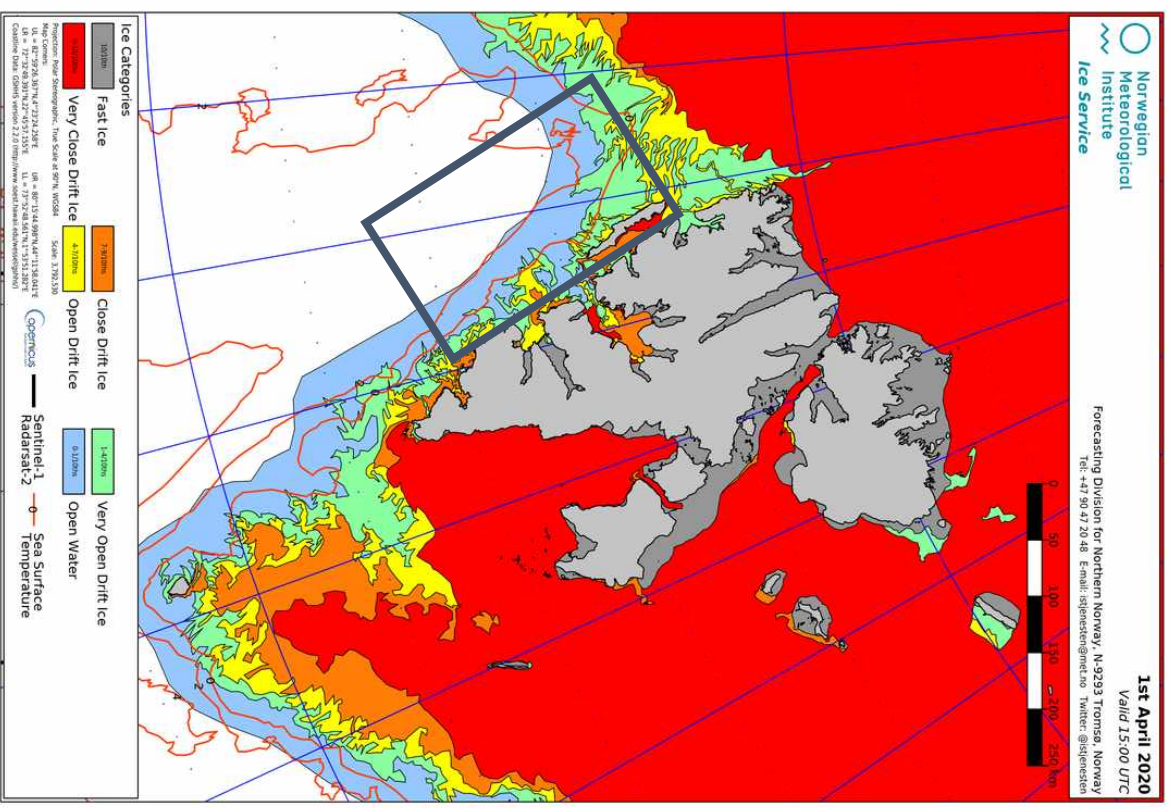Figure A 9: Ice map Svalbard 26th March 2020. Raudfjorden 010 (grey framed).

Figure A 10: Ice map Svalbard 1st April 2020. Westcoast 000, 014, 015 (grey framed).

8 Acknowledgements – Danksagung

Ein besonderer Dank geht an **Dr. Felix Christopher Mark.**

Danke Dir lieber Felix für deine Unterstützung, dein Verständnis und deinen langen Atem während des gesamten letzten Jahres! Deine Betreuung, sowie unsere Besprechungen, haben mich immer wieder motiviert und mein Interesse an meeresbiologischen Themen verstärkt. Merci!

Des Weiteren würde ich mich gerne bei **Andrea Eschbach** bedanken.

Danke Andrea für deine tatkräftige Unterstützung und Einarbeitung im Labor, sowie dein immer offenes Ohr! Es hat Spaß gemacht!

Ein herzliches Dankeschön geht an **Dr. Christoph Held.**

Danke Christoph, dass ich meine Versuche in eurem Labor durchführen konnte. Deine Tipps und Beratungen haben mir immer sehr geholfen!

Ebenfalls möchte ich **Annegret Müller** danken.

Danke Anne für deine Unterstützung und dein Interesse an meiner Arbeit.

Zu guter Letzt, würde ich mich gerne bei meinen Freunden und Freundinnen bedanken, die mich immer wieder aufgebaut und motiviert haben!